apoptotic cells with remarkably elevated PS levels. They estimated that, using the liposomes containing PS and PC (1:1), the absolute amounts of PS required for phagocytosis by 5×10^4 macrophages (the threshold of macrophage sensitivity) was 7 pmol. This value of the PS amount for 10^6 macrophages (i.e. 140 pmol) approximates to the normalized value of the PS amount for 10^6 microglial cells, which was found to be considerably effective in our study (i.e. 75 pmol). Taken together, these findings suggest that microglia also require the relatively high phospholipids concentration to recognize PS/PC liposomes as apoptotic cells. Accordingly, new techniques to ameliorate the stability of PS/PC liposomes and thus reduce the effective phospholipids concentration are called for based on the findings of *in vivo* studies.

Acknowledgements

This study was supported by a grant from Inogashira Hospital (SH). We thank Prof. Yukihiro Shoyama and Dr. Satoshi Morimoto, Department of Plant Resources Regulation, Graduate School of Pharmaceutical Sciences, Kyushu University, for technical advice about preparing liposomes.

References

Ajmone-Cat, M.A., De Simone, R., Nicolini, A., Minghetti, L., 2003. Effects of phosphatidylserine on p38 mitogen activated protein kinase, cyclic AMP responding element binding protein and nuclear factor-kappa B activation in resting and activated microglial cells. J. Neurochem. 84, 413–416.

Beckman, J.S., 1994. Peroxynitrite versus hydroxyl radical: the role of nitric oxide in superoxide-dependent cerebral injury. Ann. N.Y. Acad. Sci. 738, 69–75.

Borisenko, G.G., Matsura, T., Liu, S.X., Tyurin, V.A., Jianfei, J., Serinkan, F.B., Kagan, V.E., 2003. Macrophage recognition of externalized phosphatidylserine and phagocytosis of apoptotic Jurkat cells—existence of a threshold. Arch. Biochem. Biophys. 413, 41–52.

Chang, R.C., Rota, C., Glover, R.E., Mason, R.P., Hong, J.S., 2000. A novel effect of an opioid receptor antagonist, naloxone, on the production of reactive oxygen species by microglia: a study by electron paramagnetic resonance spectroscopy. Brain Res. 854, 224–229.

Colton, C.A., Snell, J., Chernyshev, O., Gilvert, D.L., 1994. Induction of superoxide anion and nitric oxide production in cultured microglia. Ann. N.Y. Acad. Sci. 738, 54–63.

Colton, C.A., Chernyshev, O.N., 1996. Inhibition of microglial superoxide anion production by isoproterenol and dexamethasone. Neurochem. Int. 29, 43–53.

Combs, C.K., Karlo, J.C., Kao, S.C., Landreth, G.E., 2001. Beta-amyloid stimulation of microglia and monocytes results in TNF alpha-dependent expression of inducible nitric oxide synthase and neuronal apoptosis. J. Neurosci. 21, 1179–1188.

De Simone, R., Ajmone-Cat, M.A., Nicolini, A., Minghetti, L., 2002. Expression of phosphatidylserine receptor and down-regulation of pro-inflammatory molecule production by its natural ligand in rat microglial cultures. J. Neuropathol. Exp. Neurol. 61, 237–244.

Fadok, V.A., Voelker, D.R., Campbell, P.A., Cohen, J.J., Bratton, D.L., Henson, P.M., 1992. Exposure of phosphatidylserine on the surface of apoptotic lymphocytes triggers specific recognition and removal by macrophages. J. Immunol. 148, 2207–2216.

Fadok, V.A., Bratton, D.L., Konowal, A., Freed, P.W., Westcott, J.Y., Henson, P.M., 1998. Macrophages that have ingested apoptotic cells in vitro inhibit proinflammatory cytokine production through autocrine/paracrine mechanisms involving TGF-beta, PGE2, and PAF. J. Clin. Invest. 101, 890–898.

Fadok, V.A., Bratton, D.L., Rose, D.M., Pearson, A., Ezekewitz, R.A., Henson, P.M., 2000. A receptor for phosphatidylserine-specific clearance of apoptotic cells. Nature 405, 85–90.

Hashioka, S., Monji, A., Ueda, T., Kanba, S., Nakanishi, H., 2005. Amyloid-beta fibril formation is not necessarily required for microglial activation by the peptides. Neurochem. Int. 47, 369–376.

Herrera-Molina, R., von Bernhardi, R., 2005. Transforming growth factor-beta 1 produced by hippocampal cells modulates microglial reactivity in culture. Neurobiol. Dis. 19, 229–236.

Kanzawa, T., Sawada, M., Kato, M., Yamamoto, K., Mori, H., Tanaka, R., 2000. Differentiated regulation of allo-antigen presentation by different types of murine microglial cell lines. J. Neurosci. Res. 62, 383–388.

Koistinaho, M., Koistinaho, J., 2002. Role of p38 and p44/42 mitogen-activated protein kinases in microglia. Glia 40, 175–183.

Li, J., Baud, O., Vartanian, T., Volpe, J.J., Rosenberg, P.A., 2005. Peroxynitrite generated by inducible nitric oxide synthase and NADPH oxidase mediates microglial toxicity to oligodendrocytes. Proc. Natl. Acad. Sci. U.S.A. 102, 9936–9941.

Liu, J.S., Zhao, M.L., Brosnan, C.F., Lee, S.C., 2001. Expression of inducible nitric oxide synthase and nitrotyrosine in multiple sclerosis lesions. Am. J. Pathol. 158, 2057–2066.

McGeer, P.L., Itagaki, S., Boyes, B.E., McGeer, E.G., 1988. Reactive microglia are positive for HLA-DR in the substantia nigra of Parkinson's and Alzheimer's disease brains. Neurology 38, 1285–1291.

McGeer, P.L., McGeer, E.G., 2002. Inflammatory processes in amyotrophic lateral sclerosis. Muscle Nerve 26, 459–470.

Meda, L., Cassatella, M.A., Szendrei, G.I., Otvos Jr., L., Baron, P., Villalba, M., Ferrari, D., Rossi, F., 1995. Activation of microglial cells by beta-amyloid protein and interferon-gamma. Nature 374, 647–650.

Mojovic, M., Vuletic, M., Bacic, G.G., 2005. Detection of oxygen-centered radicals using EPR spin-trap DEPMPO: the effect of oxygen. Ann. N.Y. Acad. Sci. 1048, 471–475.

Morris, R.H., Price, A.J., Tonks, A., Jackson, S.K., Jones, K.P., 2000. Prostaglandin E2 and tumour necrosis factor-alpha release by monocytes are modulated by phospholipids. Cytokine 12, 1717–1719.

Navarro-Antolin, J., Lopez-Munoz, M.J., Soria, J., Lamas, S., 2002. Superoxide limits cyclosporine-A-induced formation of peroxynitrite in endothelial cells. Free Radic. Biol. Med. 32, 702–711.

Navikas, V., Link, H., 1996. Review: cytokines and the pathogenesis of multiple sclerosis. J. Neurosci. Res. 45, 322–333.

Nishikawa, K., Arai, H., Inoue, K., 1990. Scavenger receptor-mediated uptake and metabolism of lipid vesicles containing acidic phospholipids by mouse peritoneal macrophages. J. Biol. Chem. 265, 5226–5231.

Okada, M., Irie, S., Sawada, M., Urae, R., Urae, A., Iwata, N., Ozaki, N., Akazawa, H., Nakanishi, H., 2003. Pepstatin A induces extracellular acidification distinct from aspartic protease inhibition in microglial cell lines. Glia 43, 167–174.

O'Shea, R.D., Lau, C.L., Farso, M.C., Diwakarla, S., Zagami, C.J., Svendsen, B.B., Feeney, S.J., Callaway, J.K., Jones, N.M., Pow, D.V., Danbolt, N.C., Jarrott, B., Beart, P.M., 2006. Effects of lipopolysaccharide on glial phenotype and activity of glutamate transporters: evidence for delayed up-regulation and redistribution of GLT-1. Neurochem. Int. 48, 604–610.

Possel, H., Noack, H., Keilhoff, G., Wolf, G., 2002. Life imaging of peroxynitrite in rat microglial and astroglial cells: role of superoxide and antioxidants. Glia 38, 339–350.

Qin, L., Liu, Y., Cooper, C., Liu, B., Wilson, B., Hong, J.S., 2002. Microglia enhance beta-amyloid peptide-induced toxicity in cortical and mesencephalic neurons by producing reactive oxygen species. J. Neurochem. 83, 973–983.

Qin, L., Liu, Y., Wang, T., Wei, S.J., Block, M.L., Wilson, B., Liu, B., Hong, J.S., 2004. NADPH oxidase mediates lipopolysaccharide-induced neurotoxicity and proinflammatory gene expression in activated microglia. J. Biol. Chem. 279, 1415–1421.

Qin, L., Block, M.L., Liu, Y., Bienstock, R.J., Pei, Z., Zhang, W., Wu, X., Wilson, B., Burka, T., Hong, J.S., 2005. Microglial NADPH oxidase is a novel target for femtomolar neuroprotection against oxidative stress. FASEB J. 19, 550–557.

Rivest, S., 2003. Molecular insights on the cerebral innate immune system. Brain Behav. Immunol. 17, 13–19.

Sankarapandi, S., Zweier, J.L., Mukherjee, G., Quinn, M.T., Huso, D.L., 1998. Measurement and characterization of superoxide generation in microglial cells: evidence for an NADPH oxidase-dependent pathway. Arch. Biochem. Biophys. 353, 312–321.

Shi, H., Timmins, G., Monske, M., Burdick, A., Kalyanaraman, B., Liu, Y., Clement, J.L., Burchiel, S., Liu, K.J., 2005. Evaluation of spin trapping agents and trapping conditions for detection of cell-generated reactive oxygen species. Arch. Biochem. Biophys. 437, 59–68.

Suuronen, T., Huuskonen, J., Nuutinen, T., Salminen, A., 2006. Characterization of the pro-inflammatory signaling induced by protein acetylation in microglia. Neurochem. Int. 49, 610–618.

Szelenyi, J., Selmeczy, Z., Brozik, A., Medgyesi, D., Magocsi, M., 2006. Dual beta-adrenergic modulation in the immune system: stimulus-dependent effect of isoproterenol on MAPK activation and inflammatory mediator production in macrophages. Neurochem. Int. 49, 94–103.

Tanaka, M., Sotomatsu, A., Yoshida, T., Hirai, S., Nishida, A., 1994. Detection of superoxide production by activated microglia using a sensitive and specific chemiluminescence assay and microglia-mediated PC12h cell death. J. Neurochem. 63, 266–270.

Tonks, A., Parton, J., Tonks, A.J., Morris, R.H., Finall, A., Jones, K.P., Jackson, S.K., 2005. Surfactant phospholipid DPPC downregulates monocyte respiratory burst via modulation of PKC. Am. J. Physiol. Lung Cell Mol. Physiol. 288, L1070–L1080.

Torreilles, F., Salman-Tabcheh, S., Guerin, M., Torreilles, J., 1999. Neurodegenerative disorders: the role of peroxynitrite. Brain Res. Rev. 30, 153–163.

Xie, Z., Wei, M., Morgan, T.E., Fabrizio, P., Han, D., Finch, C.E., Longo, V.D., 2002. Peroxynitrite mediates neurotoxicity of amyloid beta-peptide 1-42 and lipopolysaccharide-activated microglia. J. Neurosci. 22, 3484–3492.

Yoshida, T., Tanaka, M., Okamoto, K., 2001. Inhibitory effect of nicergoline on superoxide generation by activated rat microglias measured using a simple chemiluminescence method. Neurosci. Lett. 297, 5–8.

Zhang, J., Fujii, S., Wu, Z., Hashioka, S., Tanaka, Y., Shiratsuchi, A., Nakanishi, Y., Nakanishi, H., 2005. Involvement of COX-1 and up-regulated prostaglandin E synthases in phosphatidylserine liposome-induced prostaglandin E2 production by microglia. J. Neuroimmunol. 172, 112–120.

Available online at www.sciencedirect.com

ScienceDirect

Free Radical Biology & Medicine 42 (2007) 945–954

www.elsevier.com/locate/freeradbiomed

Original Contribution

Phosphatidylserine and phosphatidylcholine-containing liposomes inhibit amyloid β and interferon-γ-induced microglial activation

Sadayuki Hashioka [a,b,*,1], Youn-Hee Han [c,2], Shunsuke Fujii [b,3], Takahiro Kato [a], Akira Monji [a,*], Hideo Utsumi [c], Makoto Sawada [d], Hiroshi Nakanishi [b], Shigenobu Kanba [a]

[a] *Department of Neuropsychiatry, Graduate School of Medical Sciences, Kyushu University, Fukuoka, 812-8582 Japan*
[b] *Laboratory of Oral Aging Science, Faculty of Dental Sciences, Kyushu University, Fukuoka, 812-8582 Japan*
[c] *Department of Chemo-Pharmaceutical Sciences, Graduate School of Pharmaceutical Sciences, Kyushu University, Fukuoka, 812-8582 Japan*
[d] *Department of Brain Life Science, Research Institute of Environmental Medicine, Nagoya University, Japan*

Received 21 September 2006; revised 16 November 2006; accepted 5 December 2006
Available online 9 December 2006

Abstract

There is increasing evidence that microglial activation is one of the major pathogenic factors for Alzheimer's disease (AD) and the inhibition of the inflammatory activation of the microglia thus appears to be neuroprotective and a potentially useful treatment for AD. Phospholipids such as phosphatidylserine (PS) and phosphatidylcholine (PC) have been reported to modulate the immune function of phagocytes. In addition, PS has been reported to be a nootropics that can be used as nonprescription memory or cognitive enhancers. We therefore evaluated the effects of liposomes, which comprise both PS and PC (PS/PC liposomes), on the microglial production of tumor necrosis factor-α (TNF-α), nitric oxide (NO), and superoxide ($^{\bullet}O_2^-$) induced by amyloid β (Aβ) and interferon-γ (IFN-γ). Pretreatment of microglia with PS/PC liposomes considerably inhibited the TNF-α, NO and $^{\bullet}O_2^-$ production induced by Aβ/IFN-γ. These results suggest that PS/PC liposomes have both neuroprotective and antioxidative properties through the inhibition of microglial activation, thus supporting the nootropic and antidementia effect of PS.

Keywords: Alzheimer's disease; Microglia; Phosphatidylserine; Phosphatidylcholine; Nitric oxide; Superoxide; Peroxynitrite; Electron spin resonance

Introduction

Alzheimer's disease (AD) is the most common neurodegenerative disease known to cause progressive memory loss and confusion. Recently, much attention has been paid to microglial activation as a major pathogenic factor for AD. Senile plaque is the site of inflammatory processes, as evidenced by the presence of degenerating neurons and numerous reactive microglia and astrocytes associated with such plaques [1]. Microglial activation has been reported to be a relatively early pathogenetic event which precedes the process of neuropil destruction in AD patients [2]. According to in vitro studies, the microglia activated by amyloid β peptides (Aβ) have been well reported to damage or kill neurons by the excessive release of inflammatory and potentially neurotoxic molecules such as proinflammatory cytokines [e.g., tumor necrosis factor-α (TNF-α), intrleukin-1β], reactive oxygen species (ROS), and reactive nitrogen species

Abbreviations: Aβ, amyloid beta; AD, Alzheimer's disease; DEPMPO, 5-(diethoxyphosphoryl)-5-methyl-1-pyroline-*N*-oxide; ESR, electron spin resonance; IFN-γ, interferon-γ; LPS, lipopolysaccharide; MAPK, mitogen-activated protein kinase; NADPH oxidase, nicotinamide adenine diphosphate reduced form oxidase; NO, nitric oxide; PS, phosphatidylserine; PC, phosphatidylcholine; ROS, reactive oxygen species; SDS, sodium dodecyl sulfate; SOD, superoxide dismutase; TNF-α, tumor necrosis factor-α.

* Corresponding authors. S. Hashioka is to be contacted at Department of Neuropsychiatry, Graduate School of Medical Sciences, Kyushu University, Fukuoka, 812-8582 Japan. Fax: +1 604 822 7086. A. Monji, fax: +81 92 642 5644.

E-mail addresses: hashioka@interchange.ubc.ca (S. Hashioka), amonji@hf.rim.or.jp (A. Monji).

[1] Present affiliation: Kinsmen Laboratory of Neurological Research, Department of Psychiatry, Faculty of Medicine, University of British Columbia, 2255 Wesbrook Mall, Vancouver, B.C., V6T 1W5 Canada.

[2] Present affiliation: Department of Civil and Environmental Engineering, Tohoku Gakuin University, Japan.

[3] Present affiliation: Central Pharmaceutical Research Institute, JT Inc., Japan.

0891-5849/$ - see front matter © 2007 Elsevier Inc. All rights reserved.
doi:10.1016/j.freeradbiomed.2006.12.003

[i.e., superoxide radical ($^{\bullet}O_2^-$) and nitric oxide (NO), respectively] [3–6]. Peroxynitrite ($ONOO^-$), the reaction product of $^{\bullet}O_2^-$ and NO, is a highly reactive oxidant and has recently been demonstrated to act as a major mediator in the neurotoxicity induced by Aβ-activated microglia in vitro [7]. Indeed, the levels of nitrotyrosine, which is a product of the reaction of $ONOO^-$ with tyrosine residues and considered as a permanent footprint of $ONOO^-$, have been reported to increase in AD brains [8]. Taken together, the inhibition of Aβ-induced microglial production of inflammatory cytokines including TNF-α and free radicals such as NO, $^{\bullet}O_2^-$, and subsequent formation of $ONOO^-$ appears to be neuroprotective and a potentially useful treatment for AD.

Phospholipids such as phosphatidylserine (PS) and phosphatidylcholine (PC) have been shown to modulate the immune functions of phagocytes. PC, a major component of the outer leaflet of plasma membrane, has been demonstrated to reduce the production of ROS in lipopolysaccharide (LPS)/phorbol 12-myristate-13-acetate (PMA)-activated monocytes [9]. On the other hand, abnormal exposure of PS, which is normally sequestered in the inner leaflet of plasma membrane, in the early phase of apoptosis is an essential determinant for the recognition and ingestion of apoptotic cells by phagocytes [10]. After the engulfment of apoptotic cells, macrophages are well known to actively suppress the inflammatory response through the release of anti-inflammatory mediators, thereby decreasing the secretion of various proinflammatory cytokines [11]. Furthermore, PS-containing liposomes have been shown to mimic the effects of apoptotic cells on macrophages [12] and on microglia [13,14] through surface molecules that recognize PS. Intriguingly, PS has also been reported to be one of the nootropics that can be used as nonprescription memory or cognitive enhancers [15]. According to in vivo studies, PS treatment has been demonstrated to ameliorate the impaired functions of learning and memory on a variety of tasks in aged rats [16] and PS-containing liposomes have been shown to protect LPS-induced impairment of long-term potentiation (LTP) in adult rats [17]. In human clinical trials, some studies have shown that the oral administration of bovine brain cortex-derived PS improves the behavior and cognitive performances of patients with senile dementia [18,19].

For the above-noted reasons, we evaluated the effects of liposomes comprising PS and PC on the Aβ and interferon-γ (IFN-γ)-induced microglial production of proinflammatory molecules such as TNF-α, NO, and $^{\bullet}O_2^-$. Especially, $^{\bullet}O_2^-$ is a key molecule in the oxidative stress involved in the pathogenesis of AD because $^{\bullet}O_2^-$ is not only a tally of NO for $ONOO^-$ formation but also a limiting factor for $ONOO^-$ formation [20,21]. Furthermore, $^{\bullet}O_2^-$ is a precursor of other types of ROS such as hydrogen peroxide (H_2O_2) and hydroxyl radical ($^{\bullet}OH$), and ROS has also been reported to mediate proinflammatory signaling in activated microglia, thereby amplifying the TNF-α production [22]. We, therefore, measured the microglial $^{\bullet}O_2^-$ production specifically and directly using electron spin resonance (ESR) with the spin-trap technique. To our knowledge, this is the first report to directly trap $^{\bullet}O_2^-$ associated with Aβ-stimulated microglia.

Materials and methods

Aβ peptides

The Aβ25–35 peptides used in this study were purchased from AnaSpec (San Jose, CA). Purity was certified by high-performance liquid chromatography–mass spectrometry for each of the peptide. The peptides were resuspended in sterile double-deionized water, aliquoted at 5 mg/ml, and kept at −20°C. We preliminarily confirmed that neither PS/PC liposomes (data not shown) nor IFN-γ [4] affected the amyloid fibril structure of the Aβ25–35 peptides using a thioflavine-T fluorometric assay.

Chemicals and reagents

A spin-trap 5-(diethoxyphosphoryl)-5-methyl-1-pyroline-*N*-oxide (DEPMPO), LPS, and diethylenetriamine pentaacetic acid (DTPA) were purchased from Sigma Chemicals (St. Louis, MO). Superoxide dismutase (SOD; from bovine erythrocytes, 3500 U/mg), catalase (from beef liver, 11500 U/mg), xanthine, and xanthine oxidase were purchased from Wako (Osaka, Japan). The final concentrations of SOD and catalase correspond to the enzyme activities per volume as described in a previous report [23]. Recombinant IFN-γ was purchased from Genzyme (Cambridge, MA). Recombinant mouse granulocyte macrophage colony stimulating factor (GM-CSF) was purchased from R&D systems (Minneapolis, MN). Porcine brain-derived-L-α-PS, egg-derived-L-α-PC, 4-nitrobenz-2-oxa-1,3-diazole (NBD)-labeled PS, and NBD-labeled PC were purchased from Avanti Polar Lipids (Alabaster, AL).

Preparation of liposomes

The liposomes were prepared as previously described [24]. In brief, a mixture of 12 mM PS and 33 mM PC in chloroform was placed in a test tube. The liposomes were composed of either a combination of PS and PC at a molar ratio of 3:7 (PS:PC) (PS/PC liposomes) or PC only (PC liposomes). The solvent was removed in a rotary evaporator at 30°C under reduced pressure and then dried by a desiccator for 1 h. The desiccated lipids were dispersed with a vortex mixer in phosphate-buffered saline (PBS) (pH 7.4) to obtain a final concentration of 10 mM total lipids. The lipid suspensions were subsequently sonicated (Tomy UR-20P, Tokyo, Japan) for 10 min on ice. The liposome solutions were centrifuged and then the supernatants were used for the assays. Using either NBD-labeled PS or NBD-labeled PC, NBD-labeled PS/PC liposomes and NBD-labeled PC liposomes were prepared by the same methods as described above.

Microglial cell cultures

Primary microglial cells were isolated from mixed cell cultures from the cerebral cortex of 3-day-old Wister rats according to the methods described previously [4,25]. The cerebral cortex was minced and treated with papain (90 U/ml) and DNase (2000 U/ml) at 37°C for 15 min. The mechanically

dissociated cells were gently passed through plastic tips and seeded into plastic flasks at a density of 10^7/300 cm^2 in Eagle's minimal essential medium, 0.3% $NaHCO_3$, 2 mM glutamine, 0.2% glucose, 10 μg/ml insulin, and 10% fetal calf serum, and maintained at 37°C with 10% CO_2, 90% air atmosphere. The subsequent medium replacement was renewed twice per week. After 10–14 days of culture, floating cells and weakly attached cells on the primary cultured cell layer were isolated by gently shaking the flask for 10 min. The resulting cell suspension was transferred to a petri dish (Falcon 1001, Lincoln Park, NJ) and then allowed to adhere at 37°C. The unattached cells were removed after 25 min, and microglial cells were isolated as strongly adhering cells. About 90% of these attached cells were positive for OX42 (Serotec Ltd., Bichester, UK), a marker for macrophage/microglal cell types.

The murine microglial cell line, 6-3, was established from neonatal C57BL/6J(H-2b) mice using a nonenzymatic and non-virus-transformed procedure [26]. The 6-3 cells closely resemble primary cultured microglia [26,27]. The 6-3 cells were cultured in Eagle's minimal essential medium, 0.3% $NaHCO_3$, 2 mM glutamine, 0.2% glucose, 10 μg/ml insulin, and 10% fetal calf serum, and then maintained at 37°C with 10% CO_2, 90% air atmosphere. The amount of 1 ng/ml mouse recombinant GM-CSF was supplemented in the culture medium to maintain the 6-3 cells because these cells stopped proliferating without it [26]. The culture media were renewed twice per week.

Fluorescence microscopy

After the 3-h treatment of NBD-labeled PS/PC liposomes (100 μM) or NBD-labeled PC liposomes (100 μM), primary cultured rat microglia were mounted on coverslips at a density of 1.0×10^4 cells/ml and were fixed with 4% paraformaldehyde for 30 min at room temperature. Afterward, the images were taken at an excitation of 470 nm and an emission of 530 nm using fluorescence microscopy (Leica Microsystems DMRB, Wetzlar, Germany).

TNF-α quantification

Primary cultured rat microglial cells were plated on 96-well tissue culture plates at 6×10^4 per 150 μl per well and then were incubated in the presence or absence of 50 μM Aβ25–35 peptides and/or 100 U/ml IFN-γ at 37°C. After 24 h, the collected media were assayed for TNF-α accumulation. TNF-α released into the culture medium was measured using a rat TNF-α enzyme-linked immunosorbent assay (ELISA) kit (Biosource International, Camarillo, CA) based on the quantitative "sandwich" enzyme immunosorbent technique. The assay was carried out according to the manufacturer's protocol. The sensitivity of this assay was 4 pg/ml.

RNA isolation and semiquantitative RT-PCR

Primary cultured rat microglial cells were plated on 60-mm dishes at a density of $1.0–1.5 \times 10^6$ cells per dish and then incubated with stimuli for 4 h. Cellular mRNA from microglia was extracted and purified by a QuickPrep micro mRNA purification kit (Amersham, UK) according to the manufacturer's protocol. The mRNA was subsequently reverse-transcribed to single-stranded complimentary DNA (cDNA) by SuperScrip II (Invitrogen, Carlsbad, CA) with the gene-specific primers described below. Aliquots of the cDNAs were then used in separate PCR amplifications using *Taq* polymerase (Invitrogen). To determine the optimal conditions which allowed the signal to be in the liner portion of the amplification curve, experiments were performed under conditions in which the cycle number and template concentrations were altered. A negative control lacking the template RNA or reverse transcriptase was included in each experiment. The cDNA products of the reverse transcription reaction were denatured at 94°C for 2 min and then PCR amplifications were carried out as follows: for TNF-α (primers, sense 5′-CCC AGA CCC TCA CAC TCA GAT-3′; antisense 5′-TTG TCC CTT GAA GAG AAC CTG-3′), 35 cycles of denaturation at 94°C for 15 s, annealing at 50°C for 30 s, and extension at 72°C for 30 s; for GAPDH (primers, sense 5′-ACC ACA GTC CAT GCC ATC AC-3′; antisense 5′-TCC ACC ACC CTG TTG CTG TA-3′) as an internal standard, 30 cycles of denaturation at 94°C for 30 s, annealing at 55°C for 30 s, and extension at 72°C for 30 s. PCR products were separated electrophoretically on 2% agarose gel and stained with 0.1 μg/ml ethidium bromide, and then were subsequently visualized under UV illumination. The results of a scanning densitometric analysis (NIH Image 1.62 and Adobe Photoshop 7.0) are expressed as the relative ratio of TNF-α/GAPDH.

NO quantification

The accumulation of NO_2^-, a stable end product, extensively used as an indicator of NO production by cultured cells, was assayed by the Griess reaction. Primary cultured rat microglial cells were plated on 96-well tissue culture plates at 6×10^4 per 150 μl per well and incubated in the presence or absence of 50 μM Aβ25–35 peptides and 100 U/ml IFN-γ at 37 °C. After 72 h, the cell-free supernatants were mixed with equal amounts of Griess reagent (Dojindo, Kumamoto, Japan). Samples were incubated at room temperature for 15 min and subsequently absorbance was read at 540 nm using a plate reader (Model 550; Bio-Rad, Richmond, CA).

Western blotting for the detection of inducible NO synthase (iNOS)

6-3 microglial cells were plated on 6-well tissue culture plates at a density of $1.0–1.5 \times 10^6$ cells per well and then incubated with stimuli for 12 h. Afterward, cells were washed with PBS (pH 7.4) and lysed with sodium dodecyl sulfate (SDS)-containing sample buffer. Proteins were separated in a 7.5% SDS-polyacrylamide gel and transferred onto nitrocellulose membrane. The membrane was incubated with 5% nonfat dry milk to block nonspecific binding. Subsequently, the membrane was incubated with iNOS antibodies (1:2000, Upstate, Lake Placid, NY) and β-actin antibodies (1:1000, Abcam, Cambridge, MA). The expression of iNOS was detected using an enhanced chemiluminescence

system (Amersham). The band intensity was quantified with a densitometric scanner (LAS 1000, Fujifilm, Tokyo, Japan).

ESR spectroscopy

ESR, together with the spin-trapping agent DEPMPO was employed to accurately detect the production of $^{\bullet}O_2^-$ by activated microglia. The 6-3 microglial cells were cultured on 12-well tissue culture plates at a density of 2×10^6 cells in 400 μl of culture medium per well. The 6-3 cells were primed by 100 U/ml IFN-γ for 16 h in the presence or absence of the pretreatment with PS/PC or PC liposomes for 1 h at 37°C. Afterward, the 6-3 cells were incubated at 37°C with or without 50 μM Aβ25–35 for 30 min before beginning the detection of ESR spectra. Cell suspensions (i.e., 5×10^6 cells/ml) in the culture medium containing 50 mM DEPMPO were transferred to a standard cell capillary, and the ESR measurements were performed at room temperature right after the incubation. The ESR spectra were obtained using a JES-RE1X ESR spectrometer (JEOL, Tokyo, Japan). The instrument conditions were set as follows: magnetic field = 336.85 ± 7.5 mT, modulation amplitude = 2000, modulation width = 0.1 mT, modulation frequency = 100 kHz, time constant = 0.1 s, microwave power = 10 mW, microwave frequency = 9430 MHz, and sweep time = 2 min.

Spin trapping in the xanthine/xanthine oxidase sysytem

Xanthine oxidase (0.1 U/ml) was incubated with 0.4 mM xanthine in phosphate buffer (PB) containing 2 mM DTPA and 20 mM DEPMPO in the presence or absence of 2 mM PS/PC liposomes or PC liposomes. Xanthine oxidase was added last to the mixture to start the reaction. The ESR spectra were recorded at room temperature on a JES-RE1X ESR spectrometer. The instrument conditions were set as follows: magnetic field = 336.85 ± 7.5 mT, modulation amplitude = 500, modulation width = 0.1 mT, modulation frequency = 100 kHz, time constant = 0.03 s, microwave power = 10 mW, microwave frequency = 9430 MHz, and sweep time = 1 min.

Statistics

Values are expressed as the means ± SE. All parameters were analyzed by a one-way analysis of variance (ANOVA) followed by Fisher's PLSD post hoc test for specific comparisons. The significance was established at a level of $P < 0.05$.

Results

Confirmation of microglial phagocytosis of PS/PC liposomes

First, in order to confirm that the prepared liposomes are certainly engulfed by microglia, we treated primary cultured rat microglia with NBD-labeled PS/PC liposomes or NBD-labeled PC liposomes. After 3 h of treatment, the microglia were fixed with 4% PFA and examined by fluorescence microscopy. The fluorescent images were merged with the corresponding phase-contrast images. As shown in Fig. 1A, well-defined microglial cytoplasm was observed to fill with fluorescently labeled PS/PC liposomes (green). In contrast, few PC liposomes labeled with the fluorescence were observed in the microglial cytoplasm (Fig. 1B). These findings indicate that PS/PC liposomes, but not PC liposomes, were phagocytosed by microglia.

Effect of PS/PC liposomes on the TNF-α production by Aβ/IFN-γ-activated microglia

We next investigated the effect of PS/PC liposomes on the TNF-α production by Aβ/IFN-γ-activated microglia. The incubation of primary cultured rat microglia with 50 μM Aβ25–35 combined with 100 U/ml IFN-γ for 24 h resulted in significant increases in the accumulation of TNF-α, whereas neither Aβ25–35 alone nor IFN-γ alone were able to activate the microglia to release TNF-α (Fig. 2A). The massive increase was significantly reduced by the pretreatment with PS/PC liposomes for 1 h in a dose-dependent manner (Fig. 2A).

In line with the results on the protein levels, the suppressive effect of PS/PC liposomes on the expression of mRNA

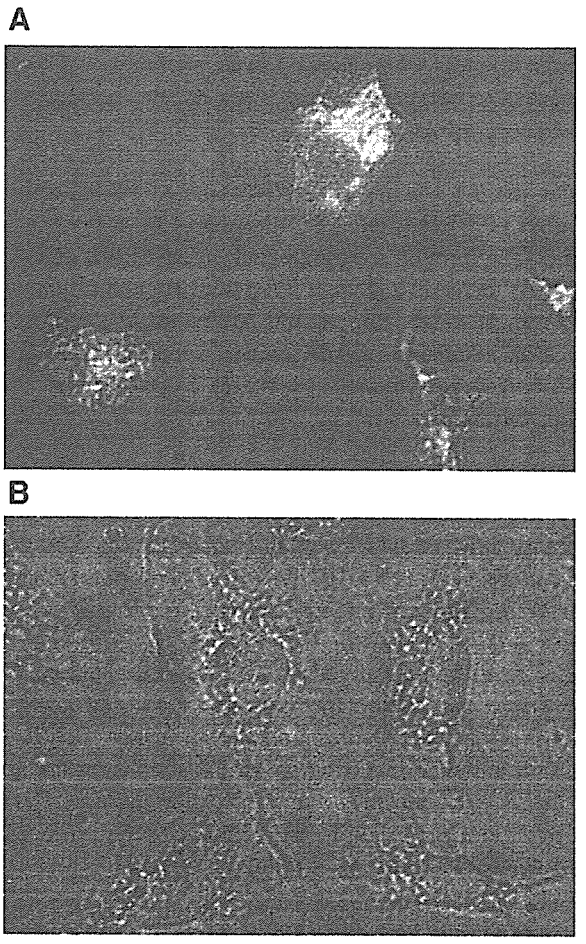

Fig. 1. Microglial phagocytosis of PS/PC liposomes. A typical fluorescence microphotograph showing phagocytosis of NBD-labeled PS/PC liposomes (green) by primary cultured rat microglia. The fluorescent image was merged with the corresponding phase-contrast image.

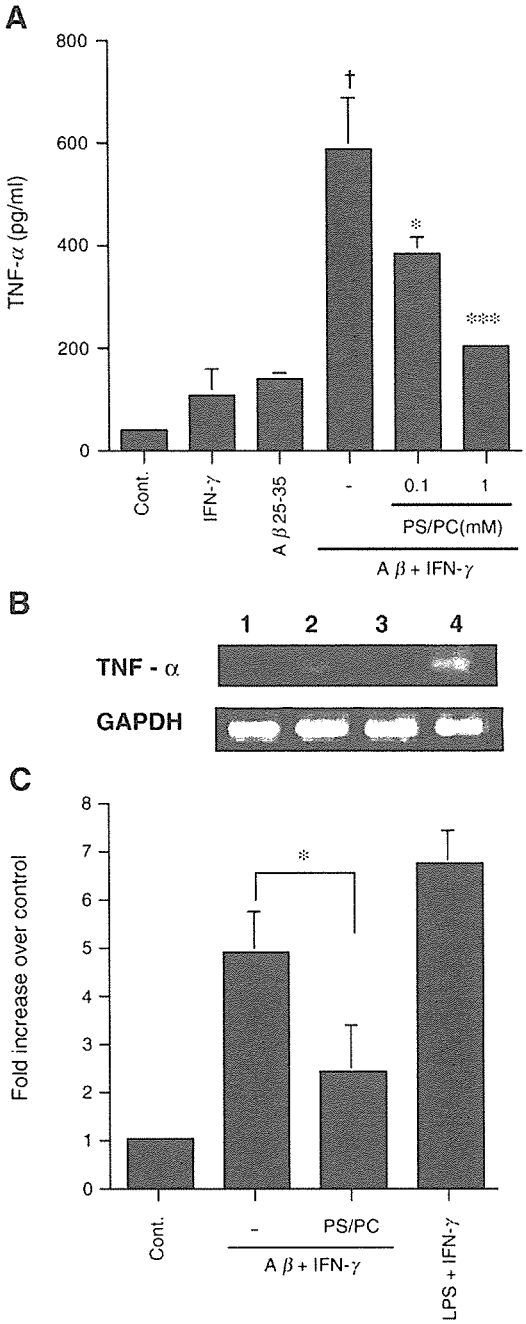

Fig. 2. Effect of PS/PC liposomes on the TNF-α production by Aβ/IFN-γ-activated microglia. (A) Primary cultured rat microglia were incubated with 50 μM Aβ25–35 and/or 100 U/ml IFN-γ at 37°C with or without pretreatment of PS/PC liposomes for 1 h. After 24 h, the collected media were assayed for TNF-α accumulation using ELISA. Data are the mean values ± SE (n=3). †P<0.0001, compared with control. *P<0.05, ***P<0.001, compared with Aβ25–35 + IFN-γ. (B) A representative RT-PCR analysis of the expression of mRNA encoding TNF-α in primary cultured rat microglia incubated with stimuli for 4 h with or without pretreatment of 1 mM PS/PC liposomes for 1 h. The administration of 10 ng/ml LPS combined with 100 U/ml IFN-γ was conducted as a positive control for the expression of TNF-α mRNA. Lane 1, control (medium); 2, Aβ25–35 + IFN-γ; 3, Aβ25–35 + IFN-γ + PS/PC liposomes; 4, LPS + IFN-γ. (C) Individual TNF-α mRNA levels were normalized to the corresponding levels of the mRNA encoding GAPDH. The results are expressed as the fold increase in the ratio of treated cell groups over the control. Data are the mean values ± SE (n = 3). *P < 0.05.

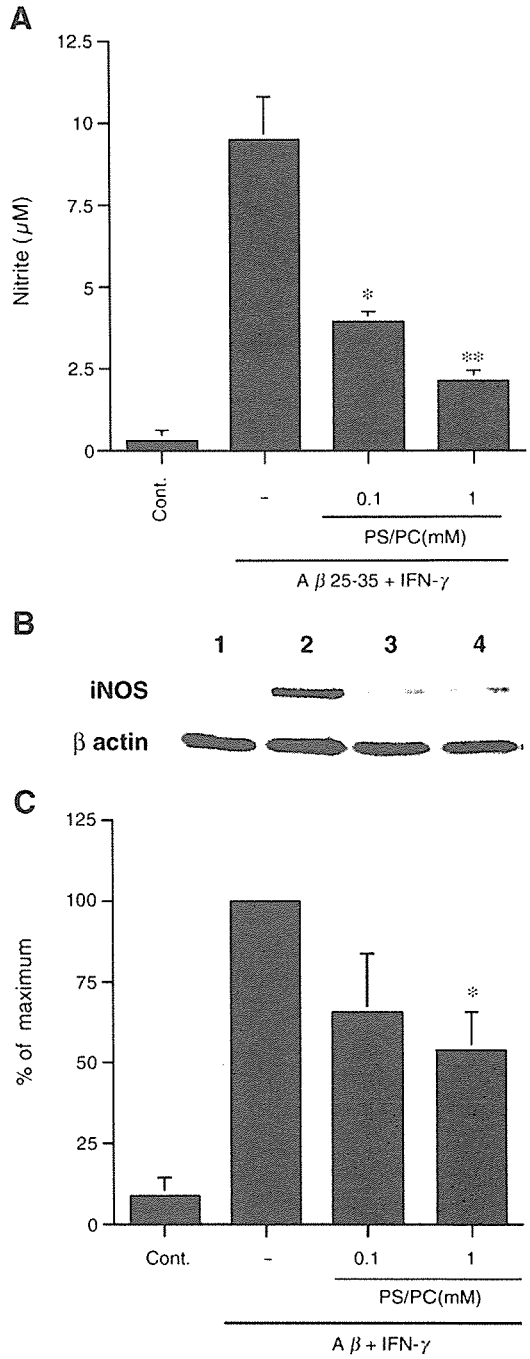

Fig. 3. Effect of PS/PC liposomes on the NO production by Aβ/IFN-γ-activated microglia. (A) Primary cultured rat microglial cells were incubated with 50 μM Aβ25–35 and 100 U/ml IFN-γ at 37°C with or without pretreatment of 1 mM PS/PC liposomes for 1 h. After 72 h, the collected media were assayed for NO accumulation using the Griess reaction. Data are the mean values ± SE. (n = 3). *P < 0.05, **P < 0.01, compared with Aβ25–35 + IFN-γ. (B) Representative Western blotting analysis of the expression of iNOS in 6-3 microglial cells incubated with Aβ25–35 + IFN-γ for 12 h with or without pretreatment of PS/PC liposomes for 1 h. Lane 1, control (medium); 2, Aβ25–35 + IFN-γ, 3, Aβ25–35 + IFN-γ + PS/PC liposomes (0.1 mM); 4, Aβ25–35 + IFN-γ + PS/PC liposomes (1 mM). (C) Individual iNOS expression levels were normalized to the corresponding levels of β-actin. The results are expressed as the percentage of the maximum levels (i.e., Aβ25–35 + IFN-γ). Data are the mean values ± SE. (n = 3). *P < 0.05 compared with Aβ25–35 + IFN-γ.

encoding TNF-α was also demonstrated by semiquantitative RT-PCR analyses. The levels of TNF-α mRNA isolated from primary cultured rat microglia incubated with 50 μM Aβ25–35 and 100 U/ml IFN-γ at 37°C for 4 h expressed approximately a fivefold rise over the nonstimulated control (Fig. 2C). The levels of increased TNF-α mRNA expression were significantly inhibited by the pretreatment with 1 mM PS/PC liposomes for 1 h to approximately two-to threefold levels of the control (Fig. 2C). The administration of 10 ng/ml LPS combined with 100 U/ml IFN-γ was conducted as a positive control for the expression of TNF-α mRNA.

Effect of PS/PC liposomes on the NO production by Aβ/IFN-γ-activated microglia

Subsequently, employing the Griess reaction assay, we investigated whether PS/PC liposomes also decrease the synthesis of NO, which is a potentially proinflammatory molecule and a tally of $^{\bullet}O_2^-$ for $ONOO^-$ formation. The incubation of primary cultured rat microglia with 50 μM Aβ25–35 combined with 100 U/ml IFN-γ at 37°C for 72 h resulted in a significant elevation in the accumulation of NO (Fig. 3A). As expected, the Aβ/IFN-γ-induced microglial NO production was significantly inhibited after 1 h of pretreatment with PS/PC liposomes in a dose-dependent manner (Fig. 3A).

We also investigated the effect of PS/PC liposomes on the NO-forming iNOS protein levels. 6-3 microglia were pretreated with PS/PC liposomes for 1 h and followed by incubation with 50 μM Aβ25–35 combined with 100 U/ml IFN-γ at 37 °C for 12 h. We observed that 1 mM PS/PC liposomes significantly downregulated the Aβ/IFN-γ-induced microglial iNOS expression (Figs. 3B and C). The PS/PC liposomes-mediated reduction of the iNOS expression was elucidated to closely parallel that of the NO levels.

Effect of PS/PC liposomes on the superoxide generation by Aβ/IFN-γ-activated microglia

Furthermore, we investigated whether or not PS/PC liposomes could suppress the generation of $^{\bullet}O_2^-$ associated with Aβ/IFN-γ-activated microglia using the ESR spin-trap

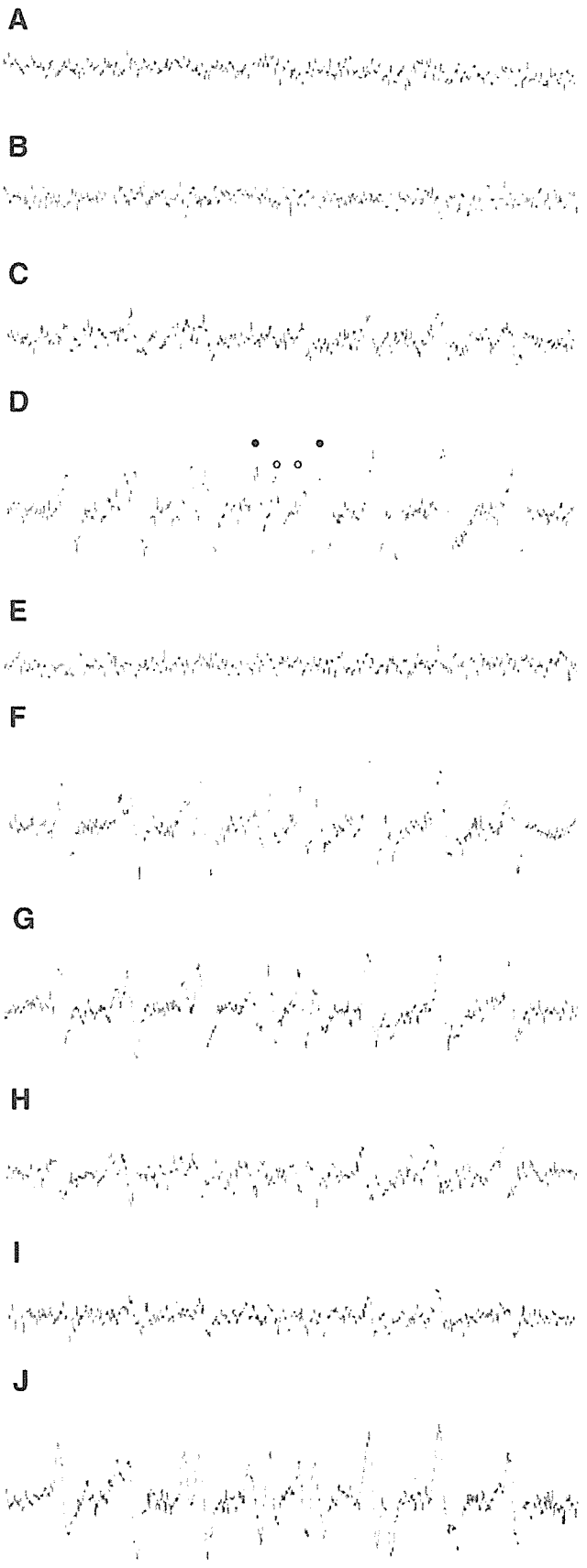

Fig. 4. Effect of PS/PC liposomes on the superoxide generation by Aβ/IFN-γ-activated microglia. 6-3 microglial cells (5×10^6/ml) were incubated with 100 U/ml IFN-γ for 16 h and 50 μM Aβ25–35 for 30 min at 37°C with or without pretreatment of PS/PC or PC liposomes for 1 h. The ESR spectra were then recorded in the presence of 50 mM DEPMPO at room temperature. (A) ESR spectra obtained from 50 μM Aβ25–35 peptide alone (cell free). (B) ESR spectra of DEPMPO adducts obtained from nonstimulated microglia. (C) ESR spectra of DEPMPO adducts obtained from the microglia stimulated by IFN-γ alone. (D) ESR spectra of DEPMPO adducts obtained from Aβ25–35/IFN-γ-activated microglia. Open and closed circles represent the measured signal peaks of DEPMPO-OH and DEPMPO-OOH adducts, respectively. (E) The same as D, but with the addition of SOD (160 μg/ml). (F) The same as D, but with the addition of catalase (280 μg/ml). (G) The same as D, but after pretreatment with PS/PC liposomes (0.5 mM) for 1 h. (H) The same as D, but after pretreatment with PS/PC liposomes (1 mM) for 1 h. (I) The same as D, but after pretreatment with PS/PC liposomes (2 mM) for 1 h. (J) The same as D, but after pretreatment with PC liposomes (2 mM) for 1 h.

technique with DEPMPO. Because several previous studies have reported spontaneously generated free radicals associated with high concentrations of Aβ peptides (i.e., millimolar order) [28,29], we beforehand confirmed that the concentrations of Aβ peptides used in this study (i.e., 50 μM) had no potency to generate $^{\bullet}O_2^-$ by itself (Fig. 4A).

In the preparations of nonstimulated 6-3 microglial cells, no signals were obtained (Fig. 4B). Microglial cells stimulated by 100 U/ml IFN-γ alone in the presence of 50 mM DEPMPO showed the weak signals whose spectra can hardly be clarified (Fig. 4C). Microglial cells stimulated by 50 μM Aβ25–35 combined with 100 U/ml IFN-γ in the presence of 50 mM DEPMPO showed prominent signals whose spectra consisted of a linear combination of a characteristic 12-line spectrum corresponding to $^{\bullet}O_2^-$ spin adduct DEPMPO-OOH and an 8-line spectrum corresponding to $^{\bullet}OH$ spin adduct DEPMPO-OH (Fig. 4D). Computer simulation confirmed DEPMPO-OOH with hyperfine splittings $a_N = 13.22$ G, $a^{\beta}{}_H = 10.962$ G, $a_p = 50.281$ G, $a^{\gamma}{}_H = 0.666$ G and DEPMPO-OH with hyperfine splittings $a_N = 12.723$ G, $a_H = 13.124$ G, $a_p = 51.119$ G. To further confirm the original species of the spin adduct generated by Aβ/IFN-γ-activated microglia, SOD (160 μg/ml) or catalase (280 μg/ml) was also treated. The ESR signal intensity substantially decreased by SOD (Fig. 4E), not by catalase (Fig. 4F). These results indicate that the spin adducts originated from the $^{\bullet}O_2^-$ radical, but not from the $^{\bullet}OH$ radical which is derived from H_2O_2. As well as an inhibitory effect of PS/PC liposomes on the TNF-α and NO production, pretreatment with PS/PC liposomes for 1 h considerably decreased the of $^{\bullet}O_2^-$ generation by Aβ/IFN-γ-activated microglia in a dose-dependent manner (Figs. 4G, H, and I). Because PC has been demonstrated to presumably act as a membrane perturber, thus reducing the production of ROS in LPS/PMA-activated monocytes [9] and in LPS/PMA-activated microglia [30], we also evaluated the effect of PC liposomes on the generation of $^{\bullet}O_2^-$ associated with Aβ/IFN-γ-activated microglia. In contrast to PS/PC liposomes, pretreatment with 2 mM PC liposomes for 1 h did not mimic the inhibitory effect of PS/PC liposomes on $^{\bullet}O_2^-$ generation of by Aβ/IFN-γ-activated microglia at all (Fig. 4J).

Effect of PS/PC liposomes on the $^{\bullet}O_2^-$ generation in the xanthine/xanthine oxidase system

To confirm whether or not the liposomes per se scavenge $^{\bullet}O_2^-$, we measured the $^{\bullet}O_2^-$ production in the xanthine/xanthine oxidase system in the presence or absence of PS/PC liposomes using ESR monitoring with a spin-trap DEPMPO. Fig. 5A shows the typical ESR spectra consisting of DEPMPO-OOH and DEPMPO-OH in the xanthine/xanthine oxidase system. The formation of these spin adducts via trapping $^{\bullet}O_2^-$ was confirmed by experiments in which SOD (160 μg/ml) was added before xanthine oxidase and ESR signals were completely quenched (data not shown), while catalase (280 μg/ml) was added, in which ESR signals were not quenched at all (data not shown). The ESR spectra in the presence of either 2 mM PS/PC liposomes were found to be essentially the same as those shown in Fig. 5A, thus indicating that PS/PC liposomes have no scavenging effect on $^{\bullet}O_2^-$, but they do have an inhibitory effect on the $^{\bullet}O_2^-$ generating system in the microglia (Fig. 5B).

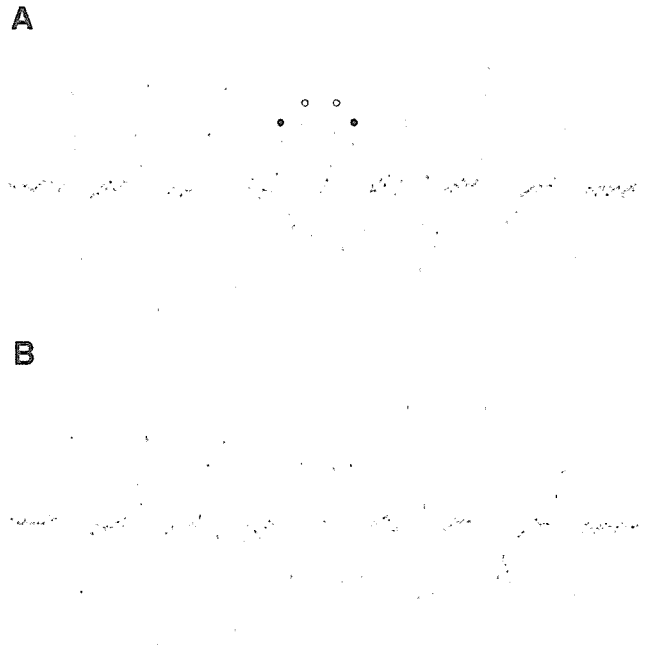

Fig. 5. Effect of PS/PC liposomes on the superoxide generation in the xanthine/xanthine oxidase system. The system contained 0.4 mM xanthine, 2 mM DTPA, and 20 mM DEPMPO in PB in the presence or absence of 2 mM PS/PC liposomes or PC liposomes. Xanthine oxidase (0.1 U/ml) was added last to the mixture in order to start the reaction. (A) ESR spectra of DEPMPO adducts obtained in the xanthine/xanthine oxidase system. Open and closed circles represent the measured signal peaks of the DEPMPO-OH and DEPMPO-OOH adducts, respectively. (B) The same as A, but in the presence of 2 mM PS/PC liposomes.

Discussion

During phagocytosis, an abrupt $^{\bullet}O_2^-$ formation called a respiratory burst occurs through activation of nicotinamide adenine diphosphate reduced form (NADPH) oxidase in phagocytes such as macrophage, neutrophils, and microglia. The $^{\bullet}O_2^-$ radical is a precursor of the microbicidal oxidants and it thus plays a crucial role in the host defense [31]. $^{\bullet}O_2^-$ is also involved in the AD pathophysiology associated with microglia-mediated neuroinflammation and oxidative stress because of $^{\bullet}O_2^-$ derivative products such as $^{\bullet}OH$ and $ONOO^-$, both of which are highly reactive and capable of exerting neurotoxicity. Especially, increasing attention has recently been paid to $ONOO^-$ as a major factor for neurotoxicity in AD pathophysiology [7,8]. Shimohama et al. have shown that the activity of NADPH oxidase is elevated in AD brains [32] and several in vitro studies have shown that Aβ activates NADPH oxidase in different cell types, thereby inducing $^{\bullet}O_2^-$ production. Specifically, Aβ25–35 has been shown to activate NADPH oxidase in human monocytes and neutrophils [33] while also inducing $^{\bullet}O_2^-$ generation in both rat microglia and human monocytes [34], and by rat peritoneal macrophages [35]. All of these studies,

however, indirectly measured the Aβ-induced $^{\bullet}O_2^-$ generation using the $^{\bullet}O_2^-$ dependent SOD-sensitive reduction of cytochrome *c*. Therefore, we directly measured the $^{\bullet}O_2^-$ generation by Aβ/IFN-γ-activated microglia using ESR with the spin-trap technique to evaluate the effect of PS/PC liposomes on microglial $^{\bullet}O_2^-$ production.

The DEPMPO is an appropriate spin-trapping agent for cell-generated $^{\bullet}O_2^-$ detection because of its stability and capability of differentiating between $^{\bullet}O_2^-$ and $^{\bullet}OH$ [36,37]. Aβ/IFN-γ-activated microglia gave rise to ESR spectra consisting of a linear combination of $^{\bullet}O_2^-$ spin adduct DEPMPO-OOH and spin adduct DEPMPO-OH. The formation of spin adducts was totally quenched by SOD but not by catalase, thus indicating that H_2O_2, which is reduced to $^{\bullet}OH$ by the Fenton reaction in the presence of Fe^{2+} or Zn^{2-}, was not a significant reactant in the formation of the observed radial signals. Moreover, the DEPMPO-OH appears to be generated by a spontaneous reduction of DEPMPO-OOH, not from H_2O_2-derived $^{\bullet}OH$ [37]. Although the noted property of DEPMPO made it possible to detect a sufficient amount of $^{\bullet}O_2^-$ to evaluate the effect of PS/PC liposomes on microglial activation in the present study, DEPMPO has recently been shown to trap $^{\bullet}O_2^-$ inefficiently in the presence of NO because the rate of the reaction between NO with $^{\bullet}O_2^-$ is faster than the rate of the reaction between DEPMPO with $^{\bullet}O_2^-$ [38]. Accordingly, the proper amount of microglial $^{\bullet}O_2^-$ generation after 16 h treatment with Aβ/IFN-γ may be larger than that demonstrated by our data under the experimental conditions supposed to induce iNOS in microglial cells.

Our data demonstrated that PS/PC liposomes have an inhibitory effect on the Aβ/IFN-γ-induced microglial production of inflammatory molecules such as TNF-α, NO, and $^{\bullet}O_2^-$, and they thus presumably prevent the subsequent formation of $ONOO^-$. Accordingly, PS/PC liposomes appear to have both neuroprotective and antioxidative properties through the inhibition of microglial activation and to be a potentially useful treatment for microglial activation-mediated neurodegenerative diseases including AD. The exact mechanism of PS/PC liposomes to suppress inflammatory activation of microglia has not yet been elucidated. De Simone et al. have indicated that the inhibitory effect of PS-containing liposomes on microglial activation is not restricted to a specific stimulant-evoked signal (s) [13]. Indeed, we previously have demonstrated that PS/PC liposomes can inhibit LPS/IFN-γ-induced microglial activation [30] as well as Aβ/IFN-γ-induced microglial activation. Consequently, PS/PC liposomes may affect various signal pathways associated with inflammatory responses in activated microglia. Ajmone-Cat et al. have shown that PS/PC-containing liposomes inhibited the phosphorylation of p38 mitogen-activated protein kinase (MAPK) and delayed that of cAMP responding element binding protein in LPS-activated microglia [39]. Because phosphorylation of p38 MAPK has been shown to mediate the signal pathway reacting for inflammatory stimulants and result in gene induction of TNF-α and NO synthase in microglia [40], the PS/PC liposomes-induced inhibition of p38 MAPK phosphorylation in activated microglia appears to suppress, at least partially, TNF-α and NO generation. Alternatively, it is also possible that the decrease in the TNF-α and NO production is a direct consequence of both decreased $^{\bullet}O_2^-$ derived ROS generation and decreased redox signaling. In support of this, there is increasing evidence that ROS can function as a second messenger to regulate several downstream molecules such as MAPKs and nuclear factor-κB (NF-κB) [41]. Indeed, it has been demonstrated that activation of NF-κB, upon which TNF-α and iNOS expression is at least partially dependent, is redox sensitive [42]. Furthermore, ROS has been reported to mediate proinflammatory signaling in LPS-activated microglia and thus amplify TNF-α production [22]. Accordingly, through directly decreasing $^{\bullet}O_2^-$ derived ROS generation, PS/PC liposomes may act indirectly to limit a wide variety of subsequent inflammatory pathways. Due to the notable role of $^{\bullet}O_2^-$ as an inflammatory enhancer as noted above, a future study investigating the effect of PS/PC liposomes on $^{\bullet}O_2^-$ forming NADPH oxidase in Aβ/IFN-γ-activated microglia is called for to clarify the $^{\bullet}O_2^-$ inhibition mechanism of PS/PC liposomes.

There is increasing evidence that TNF-α can be neuroprotective as well as neurotoxic [43]. Although the precise function of TNF-α in the pathogenesis of AD remains unclear, this cytokine might be a key mediator in modulating the microglial functions in response to Aβ [44]. In addition, a number of infiltrating T cells have been shown to increase in the brain of AD [45] and the immune cells of AD patients have the potency for overproduction of IFN-γ [46]. According to such evidence, our experimental method using IFN-γ thus seems to be consistent with the pathophysiologic microenvironment in the AD brain.

Small et al. suggested that because neuronal loss does not account, by itself, for the properties of the amnesia characteristics of AD, more attention should be paid to the effect of Aβ peptides on the synaptic function rather than on neuronal death [47]. Accordingly, the effect of PS/PC liposomes on the synaptic dysfunction caused by Aβ-induced microglial activation also needs to be confirmed in future in vivo studies, regardless PS-containing liposomes have been reported to prevent the LPS-induced impairment of LTP [17].

The total lipid concentration such as the 1 mM PS/PC liposomes used in this study certainly seems to be high. Borisenko et al., however, have suggested that phagocytes have a sensitivity threshold for PS externalized on the target cell surface which thus allows for the reliable recognition and distinction between normal cells with low amounts of externalized PS and apoptotic cells with remarkably elevated PS levels [48]. They estimated that, using the liposomes containing PS and PC (1:1), the absolute amount of PS required for phagocytosis by 5×10^4 macrophages (the threshold of macrophage sensitivity) was 7 pmol. This value of the PS amount for 10^6 macrophages (i.e., 140 pmol) approximates to the normalized value of the PS amount for 10^6 microglial cells (i.e., 60 pmol), and this value was found to be quite effective in our study. Taken together, these findings suggest that microglial cells also seem to require a relatively high phospholipid concentration to recognize PS/PC liposomes as apoptotic cells. Accordingly, new techniques to ameliorate the stability of PS/PC liposomes and reduce the effective phospholipids concentration are required for future in vivo studies.

Acknowledgments

This study was supported by a Grant-in-Aid for the Creation of Innovations through Business-Academic-Public Sector Corporation of Japan (HN), a Grant-in-Aid (15082204) (H.N.) and a Grant-in-Aid (15591230) (A.M.) for Scientific Research on Priority Areas from the Ministry of Education, Science and Culture, Japan, and a grant from Inogashira Hospital (S.H.). We thank Prof. Yukihiro Shoyama and Dr. Satoshi Morimoto, Department of Plant Resources Regulation, Graduate School of Pharmaceutical Sciences, Kyushu University, for their valuable technical advice regarding the preparation of the liposomes.

References

[1] Itagaki, S.; McGeer, P. L.; Akiyama, H.; Zhu, S.; Selkoe, D. Relationship of microglia and astrocytes to amyloid deposits of Alzheimer's disease. *J. Neuroimmunol.* **24:**173–182; 1989.

[2] Eikelenboom, P.; Bate, C.; Van Gool, W. A.; Hoozemans, J. J. M.; Rozemuller, J. M.; Veerhuis, R.; Williams, A. Neuroinflammation in Alzheimer's disease and prion disease. *Glia* **40:**232–239; 2002.

[3] Combs, C. K.; Karlo, J. C.; Kao, S. C.; Landreth, G. E. β-Amyloid stimulation of microglia, and monocytes results in TNF-α-dependent expression of inducible nitric oxide synthase and neuronal apoptosis. *J. Neurosci.* **21:**1179–1188; 2001.

[4] Hashioka, S.; Monji, A.; Ueda, T.; Kanba, S.; Nakanishi, H. Amyloid-beta fibril formation is not necessarily required for microglial activation by the peptides. *Neurochem. Int.* **47:**369–376; 2005.

[5] Meda, L.; Cassatella, M. A.; Szendrei, G. I.; Otvos Jr., L.; Baron, P.; Villalba, M.; Ferrari, D.; Rossi, F. Glial activation in Alzheimer's disease: the role of Aβ and its related proteins. *Nature* **374:**647–650; 1995.

[6] Qin, L.; Liu, Y.; Cooper, C.; Liu, B.; Wilson, B.; Hong, J. S. Microglia enhance β-amyloid peptide-induced toxicity in cortical and mesencephalic neurons by producing reactive oxygen species. *J. Neurochem.* **83:** 973–983; 2002.

[7] Xie, Z.; Wei, M.; Morgan, T. E.; Fabrizio, P.; Han, D.; Finch, C. E.; Longo, V. D. Peroxynitrite mediates neurotoxicity of amyloid β-peptides 1-42 and lipopolysaccharide-activated microglia. *J. Neurosci.* **22:**3484–3492; 2002.

[8] Smith, M. A.; Richey Harris, P. L.; Sayre, L. M.; Beckman, J. S.; Perry, G. Widespread peroxynitrite-mediated damage in Alzheimer's disease. *J. Neurosci.* **17:**2653–2657; 1997.

[9] Tonks, A.; Parton, J.; Tonks, A. J.; Morris, R. H.; Finall, A.; Jones, K. P.; Jackson, S. K. Surfactant phospholipid DPPC downregulates monocyte respiratory burst via modulation of PKC. *Am. J. Physiol. Lung Cell Mol. Physiol.* **288:**1070–1080; 2005.

[10] Fadok, V. A.; Bratton, D. L.; Henson, P. M. Phagocyte receptor for apoptotic cells: recognition, uptake, and consequences. *J. Clin. Invest.* **108:**957–962; 2001.

[11] Fadok, V. A.; Bratton, D. L.; Konowal, A.; Freed, P. W.; Westcott, J. Y.; Henson, P. M. Macrophages that have ingested apoptotic cells in vitro inhibit proinflammatory cytokine production through autocrine/paracrine mechanism involving TGF-β PGE2, and PAF. *J. Clin. Invest.* **101:** 890–898; 1998.

[12] Fadok, V. A.; Bratton, D. L.; Rose, D. M.; Pearson, A.; Ezekewitz, R. A. A receptor for phosphatidylserine-specific clearance of apoptotic cells. *Nature* **405:**85–90; 2000.

[13] De Simone, R.; Ajmone-Cat, M. A.; Nicolini, A.; Minghetti, L. J. Expression of phosphatidylserine receptor and down-regulation of proinflammatory molecule producton by its natural ligand in rat microglial cultures. *Neuropathol. Exp. Neurol.* **61:**237–244; 2002.

[14] Zhang, J.; Fujii, S.; Wu, Z.; Hashioka, S.; Tanaka, Y.; Shiratsuchi, A.; Nakanishi, Y.; Nakanishi, H. Involvement of COX-1 and up-regulated prostaglandin E synthases in phosphatidylserine liposome-induced prostaglandin E2 production by microglia. *J. Neuroimmunol.* **172:**112–120; 2005.

[15] McDaniel, M. A.; Maier, S. F.; Einstein, G. O. "Brain-specific" nutrients: a memory cure? *Nutrition* **19:**957–975; 2003.

[16] Suzuki, S.; Yamatoya, H.; Sakai, M.; Kataoka, A.; Furushiro, M.; Kudo, S. Oral administration of soybean lecithin transphosphatidylated phosphatidylserine improves memory impairment in aged rats. *J. Nutr.* **131:** 2951–2956; 2001.

[17] Nolan, Y.; Martin, D.; Campbell, V. A.; Lynch, M. A. Evidence of a protective effect of phosphatidylserine-containing liposomes on lipopolysaccharide-induced impairment of long-term potentiation in the rat hippocampus. *J. Neuroimmunol.* **151:**12–23; 2004.

[18] Delwaide, P. J.; Gyselynck-Mambourg, A. M.; Hurlet, A.; Ylieff, M. Double-blind randomized controlled study of phosphatidylserine in senile demented patients. *Acta Neurol. Scand.* **73:**136–140; 1986.

[19] Cenacchi, T.; Bertoldin, T.; Farina, C.; Fiori, M. G.; Crepaldi, G. (and participating investigators). Cognitive decline in the elderly: a double-blind, placebo-controlled multicenter study on efficacy of phosphatidylserine administration. *Aging Clin. Exp. Res.* **5:**123–133; 1993.

[20] Navarro-Antolin, J.; Lopez-Munoz, M. J.; Soria, J.; Lamas, S. Superoxide limits cyclosporine-A-induced formation of peroxynitrite in endothelial cells. *Free Radic. Biol. Med.* **32:**702–711; 2002.

[21] Possel, H.; Noack, H.; Keilhoff, G.; Wolf, G. Life imaging of peroxynitrite in rat microglial and astroglial cells: role of superoxide and antioxidants. *Glia* **38:**339–350; 2002.

[22] Qin, L.; Liu, Y.; Wang, T.; Wei, S. J.; Block, M. L.; Wilson, B.; Liu, B.; Hong, J. S. NADPH oxidase mediates lipopolysaccharide-induced neurotoxicity and proinflammatory gene expression in activated microglia. *J. Biol. Chem.* **279:**1415–1421; 2004.

[23] Chang, R. C. C.; Rota, C.; Glover, R. E.; Mason, R. P.; Hong, J. S. A novel effect of an opioid receptor antagonist, naloxone, on the product of reactive oxygen species by microglia: a study by electron paramagnetic resonance spectroscopy. *Brain Res.* **854:**224–229; 2000.

[24] Nishikawa, K.; Arai, H.; Inoue, K. Scavenger receptor-mediated uptake and metabolism of lipid vesicles containing acidic phospholipids by mouse peritoneal macrophages. *J. Biol. Chem.* **256:**5226–5231; 1990.

[25] Sastradipura, D. F.; Nakanishi, H.; Tsukuba, T.; Nishishita, K.; Sakai, H.; Kato, Y.; Gtow, T.; Uchiyama, Y.; Yamamoto, K. Identification of cellular component involved in processing of cathepsin E in primary cultures of rat microglia. *J. Neurochem.* **70:**2045–2056; 1998.

[26] Kanzawa, T.; Sawada, M.; Kato, K.; Yamamoto, K.; Mori, H.; Tanaka, R. Differentiated regulation of allo-antigen presentation by different types of murine microglial cell lines. *J. Neurosci. Res.* **62:**383–388; 2000.

[27] Sawada, M.; Imai, F.; Suzuki, H.; Hayakawa, M.; Kanno, T.; Nagatsu, T. Brain-specific gene expression by immortalized microglial cell-mediated gene transfer in the mammalian brain. *FEBS Lett.* **433:**37–40; 1998.

[28] Monji, A.; Utsumi, H.; Ueda, T.; Imoto, T.; Yoshida, I.; Hashioka, S.; Tashiro, K.; Tashiro, N. The relationship between the aggregational state of the amyloid-βpeptides and free radical generation by the peptides. *J. Neurochem.* **77:**1425–1432; 2001.

[29] Varadarajan, S.; Yatin, S.; Aksenova, M.; Jahanshahi, F.; Butterfield, D. A. Review: Alzheimer's amyloid β-peptide-associated free radical oxidative stress and neurotoxicity. *J. Struct. Biol.* **130:**184–208; 2000.

[30] Hashioka, S.; Han, Y. H.; Fujii, S.; Kato, T.; Monji, A.; Utsumi, H.; Sawada, M.; Nakanishi, H.; Kanba, S.; Phospholipids modulate superoxide and nitric oxide production by lipopolysaccharide and phorbol 12-myristate-13-acetate-activated microglia, Neurochem, Int. in press. doi:10.1016/j.neuint.2006.10.006.

[31] Ueyama, T.; Lennartz, M. R.; Noda, Y.; Kobayashi, T.; Shirai, Y.; Rikitake, K.; Yamasaki, T.; Hayashi, S.; Sakai, N.; Seguchi, H.; Sawada, M.; Sumimoto, H.; Saito, N. Superoxide production at phagosomal cup/phagosome through beta I protein kinase C during Fc gamma R-mediated phagocytosis in microglia. *J. Immunol.* **173:**4582–4589; 2004.

[32] Shimohama, S.; Tanio, H.; Kawakami, N.; Okamura, N.; Kodama, H.; Yamaguchi, T.; Nunomura, A.; Chiba, S.; Perry, G.; Smith, M. A.; Fujimoto, S. Activation of NADPH oxidase in Alzheimer's disease brains. *Biochem. Biophys. Res. Commun.* **273:**5–9; 2000.

[33] Bianca, V. D.; Dusi, S.; Bianchini, E.; Pra, I. D.; Rossi, F. Beta amyloid activates the O_2 forming NADPH oxidase in microglia,monocytes,and

neutrophils. A possible inflammatory mechanism of neuronal damage in Alzheimer's disease. *J. Biol. Chem.* **274:**15493–15499; 1999.

[34] McDonald, D. R.; Brunden, K. R.; Landreth, G. E. Amyloid fibrils activate tyrosine kinase-dependent signaling and superoxide production in microglia. *J. Neurosci.* **17:**2284–2294; 1997.

[35] Klegeris, A.; McGeer, P. L. β-Amyloid protein enhances macrophage production of oxygen free radicals and glutamate. *J. Neurosci. Res.* **49:**229–235; 1997.

[36] Shi, H.; Timmins, G.; Monske, M.; Burdick, A.; Kalyanaraman, B.; Liu, Y.; Clement, J. L.; Burchiel, S.; Liu, K. J. Evaluation of spin trapping agents and trapping conditions for detection of cell-generated reactive oxygen species. *Arch. Biochem. Biophys.* **437:**59–68; 2005.

[37] Mojovic, M.; Vuletic, M.; Bacic, G. G. Detection of oxygen-centered radicals using EPR spin-trap DEPMPO: the effect of oxygen. *Ann. N.Y. Acad. Sci.* **1048:**471–475; 2005.

[38] Pignitter, M.; Gorren, A. C.; Nedeianu, S.; Schmidt, K.; Mayer, B. Inefficient spin trapping of superoxide in the presence of nitric-oxide: implications for studies on nitric-oxide synthase uncoupling. *Free Radic. Biol. Med.* **41:**455–463; 2006.

[39] Ajmone-Cat, M. A.; De Simone, R.; Nicolini, A.; Minghetti, L. J. Effects of phosphatidylserine on p38 mitogen activated protein kinse, cyclic AMP responding element binding protein and nuclear factor-kB activation in resting and activated microglial cells. *J. Neurochem.* **84:**413–416; 2003.

[40] Koistinaho, M.; Koistinaho, J. Role of p38 and p44/42 mitogen-activated protein kinases in microglia. *Glia* **40:**175–183; 2002.

[41] Esposito, F.; Ammendola, R.; Faraonio, R.; Russo, T.; Cimino, F. Redox control of signal transduction, gene expression and cellular senescence. *Neurochem. Res.* **29:**617–628; 2004.

[42] Kaul, N.; Forman, H. J. Activation of NF kappa B by the respiratory burst of macrophages. *Free Radic. Biol. Med.* **21:**401–405; 1996.

[43] Suzuki, T.; Hide, I.; Ido, K.; Kohsaka, S.; Inoue, K.; Nakata, Y. Production and release of neuroprotective tumor necrosis factor by P2X7 receptor-activated microglia. *J. Neurosci.* **24:**1–7; 2004.

[44] Meda, L.; Baron, P.; Scarlato, G. Glial activation in Alzheimer's disease: the role of Aβ and its related proteins. *Neurobiol. Aging* **22:**885–893; 2001.

[45] Togo, T.; Akiyama, H.; Iseki, E.; Kondo, H.; Ikeda, K.; Kato, M.; Oda, T.; Tuchiya, K.; Kosaka, K. Occurrence of T cells in the brain of Alzheimer's disease and other neurological diseases. *J. Neuroimmunol.* **124:**83–92; 2002.

[46] Solerte, S. B.; Ceresini, G.; Ferrari, E.; Fioravanti, M. Hemorheological changes and overproduction of cytokines from immune cells in mild to moderate dementia of the Alzheimer's type: adverse effects on cerebromicrovascular system. *Neurobiol. Aging* **21:**271–281; 2000.

[47] Small, D. H.; Mok, S. S.; Bornstein, J. C. Alzheimer's disease and Aβtoxicity: from top to bottom. *Nat. Rev. Neurosci.* **2:**595–599; 2001.

[48] Borisenko, G. G.; Matsura, T.; Liu, S. X.; Tyurin, V. A.; Jianfei, J.; Serinkan, F. B.; Kagan, V. E. Macrophage recognition of externalized phosphatidylserine and phagocytosis of apoptotic Jurkat cells—existence of a threshold. *Arch. Biochem. Biophys.* **413:**41–52; 2003.

Journal of Cerebral Blood Flow & Metabolism (2007) 27, 488–500

www.jcbfm.com

Neuroprotective effect of exogenous microglia in global brain ischemia

Fumihiro Imai[1], Hiromi Suzuki[2], Jumpei Oda[1], Takashi Ninomiya[1], Kenji Ono[2], Hirotoshi Sano[1] and Makoto Sawada[2]

[1]*Department of Neurosurgery, Fujita Health University, Toyoake, Aichi, Japan;* [2]*Department of Brain Life Science, Research Institute of Environmental Medicine, Nagoya University, Furo-cho, Chikusa-ku, Nagoya, Aichi, Japan*

Exogenous microglia pass through the blood–brain barrier and migrate to ischemic hippocampal lesions when injected into the circulation. We investigated the effect of exogenous microglia on ischemic CA1 pyramidal neurons. Microglia were isolated from neonatal mixed brain cultures, labeled with the fluorescent dye PKH26, and injected into the subclavian artery of Mongolian gerbils subjected to ischemia reperfusion neuronal injury. PKH26-labeled microglia migrated to the ischemic hippocampal lesion, resulting in increased numbers of surviving neurons compared with control animals, even when injected 24 h after ischemia. Interferon-γ stimulation of isolated microglia enhanced the neuroprotective effect. Administration of exogenous microglia resulted in normal performance in a passive avoidance-learning task. Additionally, administration of exogenous microglia increased the expression of brain-derived neurotrophic factor and glial cell line-derived neurotrophic factor in the ischemic hippocampus, and thus might have induced neurotrophin-dependent protective activity in damaged neurons. Peripherally injected microglia exhibited a specific affinity for ischemic brain lesions, and protected against ischemic neuronal injury *in vivo*. It is possible that administration of exogenous microglia can be developed as a potential candidate therapy for central nervous system repair after transitory global ischemia.
Journal of Cerebral Blood Flow & Metabolism (2007) **27,** 488–500. doi:10.1038/sj.jcbfm.9600362; published online 5 July 2006

Keywords: blood–brain barrier; central nervous system; delayed neuronal death; drug delivery system; neurotrophic factor

Introduction

Microglia arise from the monocyte/macrophage lineage, and are ubiquitously distributed in the central nervous system, representing up to 20% of the total glial cell population in the brain (Lawson *et al*, 1990). In accordance with del Rio Hortega's early teaching (Hortega, 1932), the current view is that resident microglia are of mesodermal origin, derived from bone marrow precursor cells (Ling and Wong, 1993). These cells invade the central nervous system at an early embryonic stage to give rise to typical process-bearing microglia (Ling and Wong, 1993). Therefore, microglia may have high affinity for the brain.

Many reports describe neuron–microglia interactions after cerebral ischemia and mechanical injury (for review, see Gehrmann *et al*, 1995). It remains controversial, however, whether activated microglia promote neuronal death or neuronal survival. Many investigators maintain that microglia induce a neurotoxic effect by secreting nitric oxide (Chao *et al*, 1992) and toxic cytokines (Sawada *et al*, 1989). Moreover, microglia may contribute to the pathogenesis of neurodegeneration, such as in multiple sclerosis (Diemel *et al*, 1998), Alzheimer's disease (Barger and Harmon, 1997), and acquired immunodeficiency syndrome-associated dementia (Giulian *et al*, 1996). Conversely, other studies show that microglia protect neurons in the damaged brain by secreting cytokines, such as interleukin-1β (Giulian *et al*, 1986), interleukin-6 (Sawada *et al*, 1995), transforming growth factor-β (Suzumura *et al*, 1993),

Correspondence: Dr F Imai, Department of Neurosurgery, Fujita Health University, 1-98 Dengakugakubo, Kutsukake-cho, Toyoake, Aichi 470-1192, Japan.
E-mail: fimai@fujita-hu.ac.jp
This work was supported by a Grant-in-Aid for Scientific Research from Fujita Health University and from the 'High-Tech Research Center' Project for Private Universities: matching fund subsidy from the Ministry of Education, Culture, Sports, Science, and Technology, 2002 to 2006, Japan.
Received 13 December 2005; revised 22 May 2006; accepted 26 May 2006; published online 5 July 2006

basic fibroblast growth factor (Shimojo *et al*, 1991), hepatocyte growth factor (Hamanoue *et al*, 1996), nerve growth factor (Mallat *et al*, 1989), and tumor necrosis factor α (Sawada *et al*, 1989).

To determine whether microglia are neurotoxic or neuroprotective, they must be analyzed with *in vivo* models of neuronal injury. The role of microglia may be clarified by injecting isolated microglia at the site of neuronal injury in animal models. Direct injection of microglia into the brain, however, induces undesirable events, such as the entry of blood cells to the site of injury and immunologic responses, which complicate the analysis of the role of microglia.

Our previous studies showed that microglia isolated from rodent mixed-brain cultures retain the ability to enter the normal brain from the circulation (Imai *et al*, 1997, 1999; Sawada *et al*, 1998). Hence, microglia can be introduced into the central nervous system by injection into the bloodstream in animal models of neuronal injury. Using this system, the roles of microglia in various pathologic conditions can be analyzed.

The purpose of the present study was to evaluate whether microglia have neurotrophic or neurotoxic effects on *in vivo* brain ischemia, in which CA1 pyramidal neurons are specifically damaged. Microglia isolated from a primary culture of mixed glial cells from neonatal Mongolian gerbils were injected into the subclavian arteries of host animals subjected to ischemia reperfusion neuronal injury. We examined the number of CA1 pyramidal neurons in the brain at various time points up to 8 days. In another group of animals, we tested the effect of microglia injection on performance in a passive avoidance-learning task. We also investigated changes in the expression of brain-derived neurotrophic factor (BDNF) and glial cell line-derived neurotrophic factor (GDNF) in the ischemic hippocampus after microglia injection.

Materials and methods

Animals and Induction of Global Forebrain Ischemia

Adult male Mongolian gerbils ($n = 300$; 7 to 8 weeks old; ≈ 60 g; Seac Yoshitomi, Ltd, Fukuoka, Japan) were used in the study. Animals were housed individually, with food and water available *ad libitum*. All procedures were performed in accordance with the Guidelines for Animal Experimentation of the Fujita Health University, School of Medicine.

Ischemia was induced as described by Tone *et al* (1987). In brief, anesthesia was induced and maintained with a mixture of 2.5% halothane and nitrous oxide/oxygen (1:1). Body temperature was maintained at 37°C with a heating pad. When the spinal reflex was absent, both common carotid arteries were exposed through a ventral cervical incision and occluded with aneurysm clips for 5 mins. The clips were then released to resume normal flow to the forebrain (ISCH). Gerbils operated on without occlusion of the carotid arteries were used as controls (sham ISCH). Postoperative rectal temperature was measured three times daily (at 0700, 1400, and 2200) immediately after the induction of anesthesia with a mixture of 2.5% halothane and nitrous oxide/oxygen (1:1).

Duration of Survival Period

Ischemia was confirmed by examination of Nissl-stained brain sections 7 days after ischemia. Delayed neuronal death was observed in CA1 pyramidal neurons in all animals ($n = 20$). Approximately 2% of the animals did not survive the ischemic episode. All animals that survived were included in the data analysis. There were no differences in survival between groups.

Cell Culture

Microglia were prepared using postnatal day 1 Mongolian gerbils ($n = 200$), as described previously (Suzumura *et al*, 1984). In brief, the meninges were removed, and the brain was dissociated by passing it through a 320-μm-pore nylon mesh. After washing with Hank's balanced salt solution, the cell suspension was triturated and plated in 75-cm^2 culture flasks (Falcon 3024, Becton-Dickinson, Franklin Lakes, NJ, USA) at a density of one brain per flask in 10 mL Eagle's minimal essential medium, supplemented with 10% fetal bovine serum, 5 μg/mL bovine insulin, and 0.2% glucose. Microglia were isolated on the 14th day by the shaking off method (Suzumura *et al*, 1984). In some experiments, purified microglia were stimulated by incubation with human interferon-γ (IFNγ; Shionogi Co., Osaka, Japan) at a concentration of 5×10^3 U in 10 mL in a plastic dish at 37°C for 24 h.

Macrophages were collected by injecting 10 mL of cold (4°C) phosphate-buffered saline into the peritoneal cavities of a separate group of gerbils. Peritoneal fluid was withdrawn three times with a 21-gauge needle attached to a plastic syringe. The cells were maintained at 4°C, centrifuged at 1,000 *g* for 5 mins, and seeded onto plastic dishes containing Eagle's minimal essential medium with 10% fetal bovine serum, where they adhered for 1 h at 37°C in 5% CO_2.

PKH26 Labeling

PKH staining provides stable, clear, intense, accurate, and reproducible fluorescent labeling of live cells for an extended period of time, with no apparent toxic effects (Horan and Slezak, 1989). PKH is an aliphatic reporter molecule that is inserted into the cell membrane lipid bilayer by selective partitioning. It is effective for a variety of cell types and exhibits no significant leaking or transfer between cells. We used PKH26 to label the exogenous microglia within the brain, using a PKH26 Red Fluorescent Cell Linker Kit for Phagocytic Cell Labeling (PKH26-PCL; Sigma Chemical Co., St Louis, MO, USA). PKH26-PCL labels phagocytic cells with excitation (551 nm) and emission (567 nm) wavelengths compatible

with rhodamine or phycoerythrin detection systems. The labeling occurs through the formation of aggregates of particles. The aggregation significantly inhibits the uptake of dye by nonphagocytic cells, such as lymphocytes, but facilitates dye uptake by phagocytic cells. Labeled cells appear patchy or spotted because the dye localizes in phagocytic compartments of the cells. The dye appears to be resistant to metabolic breakdown and labels the cells for at least 21 days *in vivo*. Use of PKH26 can be combined with immunocytochemistry (Silverman *et al*, 2000), but is not suitable for double staining, because it is easily abolished by the fixation required for immunocytochemistry.

Labeling of microglia and macrophages with PKH26 was performed using the standard phagocytosis procedure of microscopic particles, according to the manufacturer's instructions. In brief, cells in a 10-cm plastic dish were incubated with PKH26 staining solution containing 10 μmol/L PKH26, 50% Diluent B (a phagocytic cell-labeling solution, Sigma Chemical Co.), and 50% culture medium for 15 mins, then washed three times in 10 mL of serum-containing medium. PKH26-stained cells were harvested using a rubber policeman in 2 mL of ice-cold phosphate-buffered saline (pH 7.2) and washed three times with 5 mL of ice-cold phosphate-buffered saline (pH 7.2) by centrifugation at 1,000 *g* for 3 mins. The cells were then resuspended in the culture medium for injection into the host.

Injection of Cells

Intraarterial cell injection was performed as described previously (Ishihara *et al*, 1993). Cells were injected either 24 h before or 24 h after ischemia was induced. In a subset of experiments, microglia were injected 48 h after ischemia induction. In brief, sham ISCH and ISCH gerbils were anesthetized with a mixture of 2.5% halothane and nitrous oxide/oxygen (1:1). When the spinal reflex was absent, a transverse incision was made under the left clavicle. The left subclavian artery was exposed and dissected from the surrounding tissues. After temporary occlusion of the subclavian artery with an aneurysm clip, a small hole was made in the distal side of the artery with a 27-gauge needle, and a polyethylene tube (Becton Dickinson, Tokyo, Japan) was inserted proximally into the hole. After the aneurysm clip was released, PKH26-labeled microglia or macrophages (0.5 mL of final suspension media estimated to contain 1×10^6 cells) were injected as a bolus for 30 secs into the subclavian artery through the polyethylene tube.

Tissue Preparation

Gerbils were deeply anesthetized with ketamine hydrochloride (60 mg/kg, intraperitoneally) and killed by transcardial perfusion with isotonic saline solution. Brains were removed, frozen in liquid nitrogen, and embedded in OTC compound (Tissue Tek, Elkhart, IN, USA). Coronal sections (8 μm thick) at the hippocampal level were cut with a cryostat, mounted on slides, and dried. To preserve PKH26 labeling, the sections were lightly fixed with 4% paraformaldehyde in 0.1 mol/L phosphate buffer, pH 7.2, for 10 mins. To determine the location of exogenous microglia relative to ischemic CA1 pyramidal neurons, an immunofluorescent study was performed using terminal deoxynucleotidyl transferase (TdT)-mediated deoxyuracil nucleotides-biotin nick-end labeling (TUNEL), *Griffonia simplifolia* B4 isolectin (IB4), and an antibody to microtubule-associated protein 2 (MAP2). To localize BDNF and GDNF expression, immunohistochemistry using the avidin–biotin complex method was performed.

TUNEL staining was used to detect DNA fragmentation in cell nuclei. The hippocampal sections were pretreated with or without 20 μg/mL proteinase K (Sigma Chemical Co.) at room temperature (RT) for 15 mins. After treatment with 0.3% H_2O_2 in methanol for 30 mins, sections were incubated with 100 U/mL TdT and 10 nmol/L per mL biotinylated 16-2′-dUTP (Boehringer-Mannheim-Yamanouchi, Tokyo, Japan) in TdT buffer (100 mmol/L sodium cacodylate, pH 7.0, 1 mmol/L cobalt chloride, and 50 μg/mL gelatin) in a humid atmosphere at 37°C for 60 mins. Further incubation with fluorescein isothiocyanate-conjugated avidin (Nichirei, Tokyo, Japan) was performed for 60 mins at RT.

Microglial cells were identified by IB4 staining. Cryosections were incubated with 20 μg/mL biotinylated IB4-fluorescein isothiocyanate conjugate (Sigma Chemical Co.) in 0.01 mol/L phosphate-buffered 0.15 mol/L saline (pH 7.2) containing 0.1% Triton X-100 at RT for 2 h (Streit, 1990).

Hippocampal CA1 pyramidal neurons were visualized using a monoclonal antibody to MAP2 (Chemicon, Temecula, CA, USA). Sections were incubated with 10% normal goat serum for 30 mins at RT. They were then incubated with a mouse monoclonal anti-MAP2 antibody, diluted 1:100, for 1 day at 4°C. Further incubations were performed with fluorescein isothiocyanate-conjugated anti-mouse IgG (Jackson ImmunoResearch Laboratories, West Grove, PA, USA), diluted 1:500, at RT for 60 mins.

We visualized BDNF epitopes using a rabbit polyclonal anti-BDNF antibody (diluted 1:500; Santa Cruz Biotechnology, Santa Cruz, CA, USA) and GDNF epitopes were visualized using a rabbit polyclonal anti-GDNF antibody (diluted 1:250; Santa Cruz Biotechnology). Sections were then incubated in secondary antibody, biotinylated goat anti-rabbit IgG, followed by avidin–biotin complex (Elite kit: Vector Laboratories, Burlingame, CA, USA), and visualized after chromogenic reaction with 3,3′-diaminobenzidine.

The sections were analyzed with an Olympus BX51 microscope equipped with bright-field and fluorescent light sources (Tokyo, Japan). Both bright-field and fluorescent images were captured from the same field using a Penguin 600 CL camera (Pixera Corporation, Los Gatos, CA, USA).

Cell Counts

Six serial, coronal frozen sections (8 μm thick) at the CA1 hippocampal level were examined. Cells were counted if

they were within a randomly selected 1-mm linear length of CA1. To determine the time course of exogenous microglia migration to the ischemic hippocampus, PKH26-labeled microglia were counted in animals injected with nonstimulated or IFNγ-stimulated microglia 24 h before ischemia, and at 2, 3, 5, and 7 days after ischemia. To determine whether exogenous microglia reduced ischemic damage caused by transient global ischemia, surviving pyramidal neurons were counted in ISCH or sham ISCH animals infused with vehicle (ISCH/VEH, SHAM/VEH), nonstimulated microglia (ISCH/Mi, SHAM/Mi), or IFNγ-stimulated microglia (ISCH/γMi, SHAM/γMi), 24 h before (PRE) or 24 h after (POST) ischemia. All neurons (cresyl violet-positive cells) with an intact morphologic appearance were counted in each animal either 7 or 14 days after ischemia. A total of 10 animals were examined for each of the 12 conditions.

Passive Avoidance Task

A step-through type passive avoidance apparatus was used to evaluate memory, as described previously (Nanri *et al*, 1998). The apparatus comprised two compartments: one light and one dark (each $16.5 \times 16.0 \times 14.7$ cm), separated by a guillotine door. The dark compartment had a stainless-steel grid floor. A scrambled electric shock was delivered through the grid floor by a shock generator (Daiichi Kikai Inc., Tokushima, Japan). The passive avoidance learning trial was performed either 7 or 14 days after inducing ischemia. At the beginning of the training session, each animal was placed in the light compartment. When the animal stepped into the dark compartment, the door between compartments was closed and a foot shock (0.6 mA, 3 secs) was delivered through the floor. The door was then opened and the animal was allowed to cross back into the light compartment. Each time the animal stepped into the dark compartment, a foot shock was delivered. Eventually, the animal remained in the light compartment. The learning trial lasted 8 mins.

The retention test was performed 24 h after the learning trial. In the retention test, the gerbil was placed in the light compartment, and the latency to enter the dark compartment was measured. If the gerbil did not enter the dark compartment within 180 secs, a score of 180 secs was assigned. Performance on the passive avoidance task was evaluated in the SHAM/VEH-(PRE/POST), ISCH/VEH-(PRE/POST), ISCH/Mi-(PRE/POST), and ISCH/γMi-(PRE/POST) groups. Ten animals were used for each of the eight conditions.

Enzyme-Linked Immunosorbent Assay

Changes in BDNF and GDNF levels were measured in the hippocampus in SHAM/VEH, ISCH/VEH, ISCH/Mi, or ISCH/γMi animals using the BDNF and GDNF Emax Immunoassay System Kit (Promega, Madison, WI, USA). In the hippocampus of ISCH/VEH-PRE or ISCH/Mi-PRE gerbils, each neurotrophic factor level was measured 2 h, 1 day, 3 days, and 7 days after inducing ischemia. In the hippocampus of ISCH/VEH-POST and ISCH/Mi-POST animals, each neurotrophic factor level was measured 26 h, 2 days, 4 days, and 8 days after ischemia. As a control, we used the hippocampus from SHAM/VEH-PRE animals, which was dissected 6 h after the treatment (Marmigere *et al*, 2003). Neurotrophic factor levels were also measured in the rest of the brain after the hippocampus was removed.

Results

Recruitment of Exogenous Microglia into CA1 Hippocampal Lesions

Figure 1 shows fluorescent staining in the hippocampal CA1 field of ISCH animals injected with PKH26-labeled exogenous microglia 24 h before ischemia. PKH26-labeled cells accumulated near TUNEL-positive cells (Figures 1A–1D). PKH26-labeled cells were also located in the vicinity of MAP2-positive pyramidal neurons 3 days after ischemia (Figure 2A). IB4 staining of adjacent sections revealed that all PKH26-labeled cells were IB4-positive (Figures 2B–2D).

PKH26-labeled cells that reacted with IB4 were identified as microglia. Most of the microglia that accumulated in the CA1 field were both PKH26- and IB4-positive exogenous microglia, whereas there were only a few PKH26-negative and IB4-positive endogenous microglia (Figures 2B–2D). The TUNEL-positive cells were probably pyramidal neurons, because they were in the CA1 pyramidal cell layer and were not labeled with PKH26 (Figures 1A–1D). Neither TUNEL-positive pyramidal neurons nor PKH26-labeled microglia were detected in CA1 1 day after ischemia (data not shown). Two days after ischemia, only a few TUNEL-positive pyramidal neurons were detected in a portion of CA1, and PKH26-labeled microglia had accumulated in or around the TUNEL-positive neurons (Figures 1A and 1B). Three days after ischemia, a few TUNEL-positive pyramidal neurons were detected in CA1 (data not shown) and PKH26-labeled microglia were scattered throughout the CA1 field (Figure 2A). Five days after ischemia, many TUNEL-positive pyramidal neurons and PKH26-labeled microglia were distributed throughout CA1. Many of these cells had accumulated near the CA1–CA2 border (Figures 1C and 1D). The number of TUNEL-positive pyramidal neurons and PKH26-labeled microglia in the CA1 layer increased in a time-dependent manner until 7 days after ischemia (Figures 1A–1D and 3A). Stimulation with IFNγ increased the number of migrating exogenous microglia in the ischemic CA1 pyramidal cell layer (Figure 3A). The temporal profile of exogenous microglia recruitment was the same if the microglia were injected after ischemia onset (data not shown). In a separate set of experiments, PKH26-labeled macrophages did not enter the brain from the circulation (data not shown).

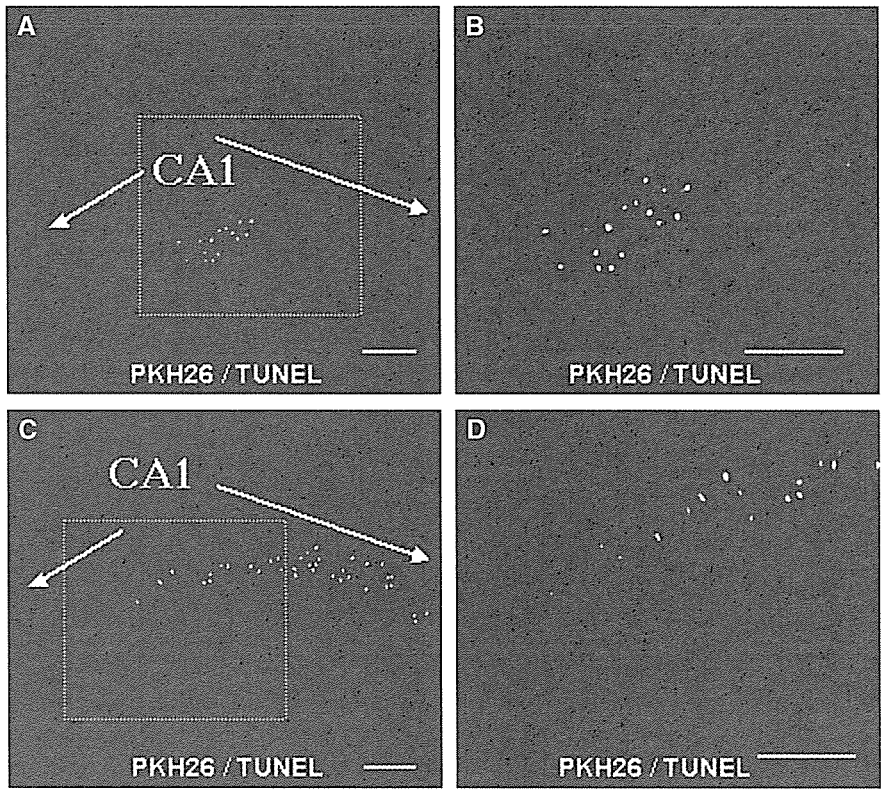

Figure 1 Migration of PKH26-labeled cells to TUNEL-positive CA1 pyramidal neurons after transient global ischemia. The panels show fluorescent staining in hippocampal CA1 sections obtained from ISCH animals injected with PKH26-labeled exogenous microglia 24 h before ischemia. (**A–D**) Double staining with PKH26 and TUNEL (PKH26/TUNEL). (**A**) Small numbers of TUNEL-positive pyramidal neurons (green) appeared in the CA1 field 2 days after ischemia. PKH26-labeled exogenous microglia (red) accumulated around TUNEL-positive pyramidal neurons (green). (**B**) Higher magnification of the boxed area in panel A. (**C**) Many TUNEL-positive pyramidal neurons (green) were present in the CA1 field 5 days after ischemia. Many PKH26-labeled exogenous microglia (red) accumulated in the ischemic CA1 field. (**D**) Higher magnification of the boxed area in panel C. (**A**, **C**) Arrows indicate the longitudinal extent of the CA1 field of the hippocampus. All scale bars = 10 μm.

Reduction of Ischemic Damage by Microglia Injection

Figure 3B shows the hippocampus from SHAM/VEH, ISCH/VEH, ISCH/Mi, and ISCH/γMi animals 7 days after ischemia. Most of the pyramidal neurons in the CA1 field had degenerated in ISCH/VEH animals. Microglial infusion (ISCH/Mi) increased the number of surviving pyramidal neurons, and IFNγ stimulation (ISCH/γMi) enhanced the microglial neuroprotective effect.

Figure 3C shows the number of surviving pyramidal neurons in the CA1 field 7 days after ischemia in SHAM/VEH, ISCH/VEH, ISCH/Mi, and ISCH/γMi animals. SHAM/VEH animals were used as controls ($n = 10$). There was no effect of injection of nonstimulated microglia or IFNγ-stimulated microglia on the number of surviving CA1 pyramidal neurons in SHAM/VEH animals (data not shown). Ischemia significantly reduced the number of surviving pyramidal neurons. Intraarterial injection of microglia (either PRE or POST) significantly increased the number of surviving neurons ($P < 0.001$). Stimulation of the microglia with IFNγ further enhanced neuron survival ($P < 0.001$). The injection of vehicle, nonstimulated microglia, or IFNγ-stimulated microglia had no effect on postoperative body temperature throughout the survival period (data not shown). The number of surviving CA1 neurons at 14 days after ischemia was not different from that at 7 days after ischemia in each study (data not shown). Injection of microglia 48 h after ischemia had no significant effect on pyramidal neuron death (data not shown). The injection of PKH26-labeled macrophages into ISCH animals had no effect on the number of surviving CA1 pyramidal neurons (data not shown).

Prevention of Ischemia-Induced Learning Impairment by Microglia Injection

The passive avoidance task was used to determine whether exogenous microglia prevent ischemia-induced learning impairment. Figure 4 shows behavioral responses from gerbils 7 days after ischemia. The mean retention latency was shorter

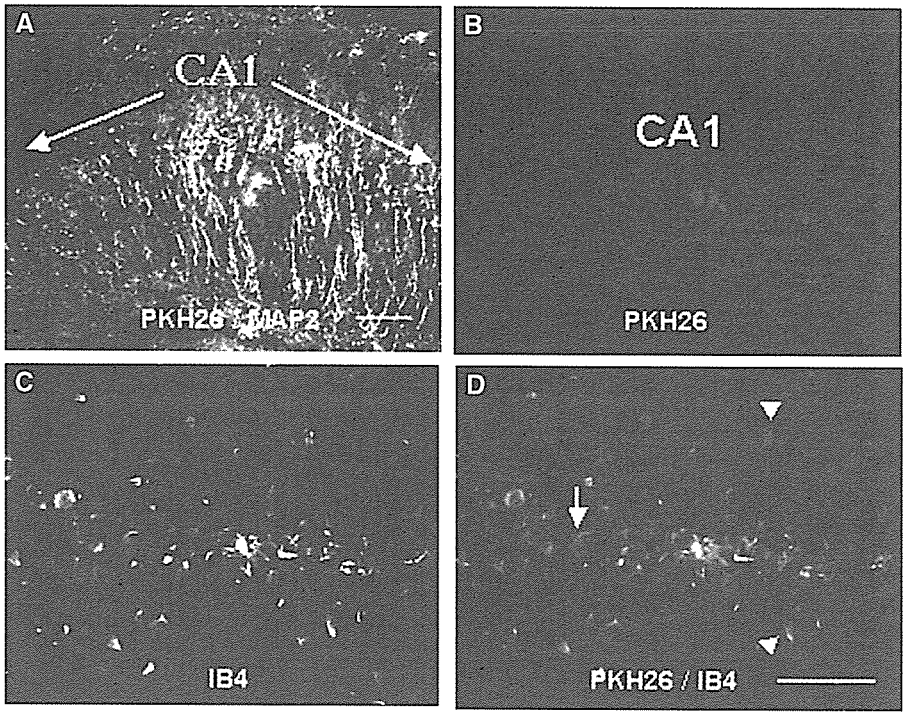

Figure 2 Migration of exogenous microglia to hippocampal CA1 lesions after transient global ischemia. The panels show fluorescent staining in hippocampal CA1 sections obtained from ISCH animals injected with PKH26-labeled exogenous microglia 24 h before ischemia. (**A**) Double staining with PKH26 and an anti-MAP2 antibody (PKH26/MAP2). Many PKH26-labeled exogenous microglia (red) were scattered around MAP2-positive pyramidal neurons (green) 3 days after ischemia. (**B**) PKH26 staining of the adjacent hippocampal section in panel A. (**C**) IB4 staining of the adjacent section. (**D**) Double staining of the adjacent section with PKH26 and IB4 (PKH26/IB4). All of the PKH26-labeled exogenous microglia (red) in the CA1 area expressed IB4 (green). A few IB4-positive and PKH26-negative endogenous microglia (arrow) were observed. Vascular endothelial cells around the hippocampus (arrowheads) also expressed IB4. Arrows in panel A indicate the longitudinal extent of the CA1 field of the hippocampus and the arrow in panel D indicates endogenous microglia. Arrowheads indicate endothelial cells. All scale bars = 10 μm.

for ISCH/VEH animals than for SHAM/VEH animals ($P<0.01$). The mean retention latency of the ISCH/Mi-PRE animals was longer than that of the ISCH/VEH-PRE animals ($P<0.01$), although the mean retention latency of the ISCH/Mi-POST animals was not different from the ISCH/VEH-POST animals. The mean retention latency was significantly longer in the ISCH/γMi-PRE ($P<0.001$) and ISCH/γMi-POST ($P<0.01$) animals (Figure 4) compared with the ISCH/VEH (PRE/POST) animals. The microglia-induced increase in the mean retention latency at 14 days after ischemia was not statistically different from the mean retention latency at 7 days after ischemia in each study (data not shown). The injection of macrophages into ISCH animals had no effect on retention latency (data not shown).

BDNF and GDNF Expression in the ISCH Hippocampus

The time course of hippocampal BDNF and GDNF expression was examined in SHAM and ISCH animals, and the effects of exogenous microglia on the expression of these neurotrophic factors was investigated. The time course of hippocampal BDNF and GDNF expression after ischemia was measured by enzyme-linked immunosorbent assay (Figure 5). In the hippocampus of ISCH animals, GDNF expression levels decreased significantly 2 h after ischemia and gradually increased during the next 7 days. In contrast, animals that received microglial injections 24 h before ischemia showed no decrease in BDNF or GDNF levels. Expression levels of BDNF remained constant until 3 days after ischemia, at which time they approximately doubled. Expression of GDNF in microglia-injected animals showed a rapid increase 2 h after ischemia and continued to increase during the course of 7 days to approximately 600% of the baseline level. There was no difference in BDNF or GDNF expression levels in animals injected with IFNγ-stimulated microglia, compared with nonstimulated microglia. Injection of microglia 24 h after ischemia induced a similar increase in BDNF and GDNF expression (Figure 5). Microglia-induced increases in neurotrophic factors were not observed except in the hippocampus (data not shown). The injection of macrophages into ISCH animals did not change BDNF or GDNF expression in the hippocampus (data not shown).

To determine which cells expressed BDNF and GDNF in our ischemia model, we examined the hippocampus using immunohistochemical analysis in SHAM/VEH, ISCH/VEH-PRE, and ISCH/Mi-PRE gerbils (Figure 6). In SHAM animals, hippocampal CA1 neurons and endogenous microglia-like cells expressed both GDNF and BDNF (Figures 6A and 6E). Two hours after ischemia, most of the CA1 neuron-like cells did not express BDNF and GDNF, and BDNF-positive endogenous microglia-like cells were scattered throughout CA1 (Figures 6B and 6F). Three days after ischemia, most CA1 neurons weakly expressed BDNF, whereas GDNF levels recovered (Figures 6C and 6G). Seven days after ischemia, BDNF immunoreactivity was detected in the CA1 neuron-like cell bodies, endogenous microglia, and also in some cell bodies and processes of reactive astrocyte-like cells near the ischemic CA1 field (Figure 6D).

At 7 days, damaged CA1 neuron-like cells expressed GDNF and many GDNF-positive, microglia-like cells were observed throughout CA1, whereas GDNF-positive, astrocyte-like cells were not detected (Figure 6H). Most of the CA1 neuron-like cells expressing BDNF or GDNF seemed to undergo degeneration because the cytoplasm was enlarged and the nucleus was not visible. Injection of microglia 24 h before ischemia greatly increased staining of BDNF- and GDNF-like immunoreactivity in CA1 neurons.

Discussion

In this study, we show that systemically injected microglia provide significant neuroprotection to the hippocampus after an ischemic insult. In addition to promoting CA1 cell survival, injection of microglia either before or 24 h after ischemia improved performance in a passive-avoidance learning task. There was also an increase in BDNF and GDNF expression in the hippocampus.

Previous studies indicate that endogenous microglia migrate to the CA1 pyramidal cell layer and protect ischemic neurons after reperfusion neuronal injury (Nitatori *et al*, 1995; Pinteaux *et al*, 2006; Neumann *et al*, 2006). In the present study, exogenous microglia migrated to areas that suffered ischemic damage, indicated by the presence of PKH26-positive cells around TUNEL-positive neurons in the CA1 pyramidal cell layer. Most of the cells were both PKH26-positive and IB4-positive exogenous microglia, although there were also a few

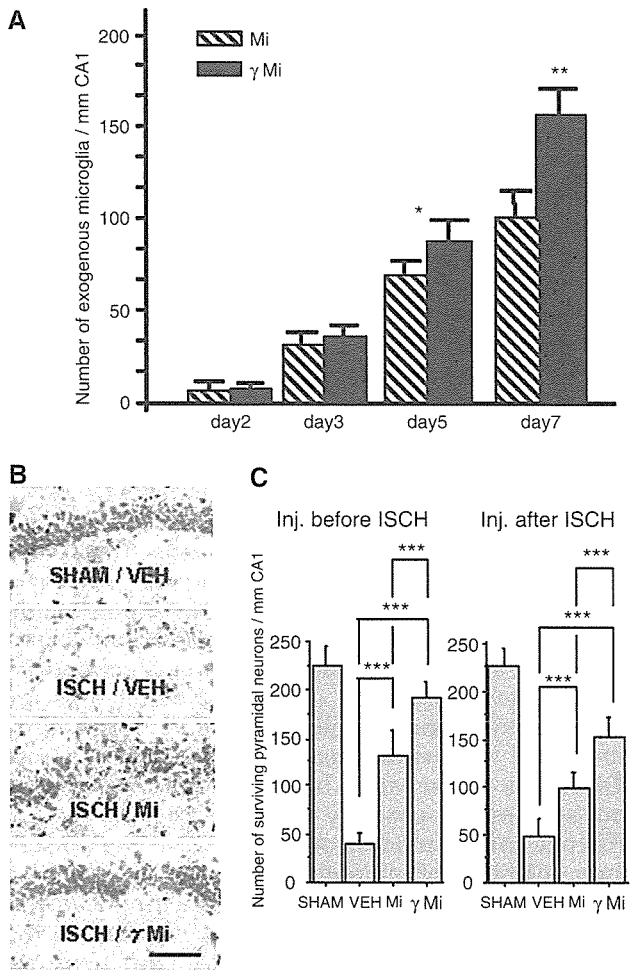

Figure 3 Neuroprotective effects of exogenous microglia. (**A**) Time course of the number of PKH26-labeled microglia migrating to the ischemic CA1 layer. Stimulation with IFNγ resulted in higher numbers of migrating microglia in the ischemic CA1 pyramidal than nonstimulated microglia. Vertical bars in each histogram indicate means $\pm$ s.d. ($n = 10$). Hatched columns (Mi) indicate the number of migrating nonstimulated microglia and black columns (γMi) indicate the number of IFNγ-stimulated microglia. $^*P < 0.05$ and $^{**}P < 0.01$, significantly different from the corresponding nonstimulated microglia-infused group (Student's *t*-test). (**B**) Photomicrographs of CA1 hippocampal sections 7 days after ischemic insult. SHAM/VEH: intraarterial injection of culture medium 24 h before sham-ischemia treatment; ISCH/VEH: intraarterial injection of culture medium 24 h before ischemia; ISCH/Mi: intraarterial injection of nonstimulated microglia 24 h before ischemia; ISCH/γMi: intraarterial injection of IFNγ-stimulated microglia 24 h before ischemia. Scale bar = 5 μm and applies to all four panels. (**C**) The number of surviving pyramidal neurons in the hippocampus 7 days after ischemia onset. Injection of microglia resulted in higher numbers of surviving pyramidal neurons after transient global ischemia (relative to ISCH/VEH), even when injections were placed 24 h after ischemia. Stimulation with IFNγ increased microglial neuroprotective effect. Vertical bars represent the mean $\pm$ s.d. ($n = 10$). $^{***}P < 0.001$, Analysis of variance with Bonferroni *post hoc* test for multiple pairwise comparisons. Inj. before ISCH: intraarterial injection 24 h before ischemia treatment; Inj. after ISCH: intraarterial injection 24 h after ischemia treatment; SHAM: injection of culture medium into sham-ischemia treated animals; VEH: injection of culture medium into ischemia-treated animals; Mi: injection of nonstimulated microglia into ischemia-treated animals; γMi: injection of IFNγ-stimulated microglia into ischemia-treated animals.

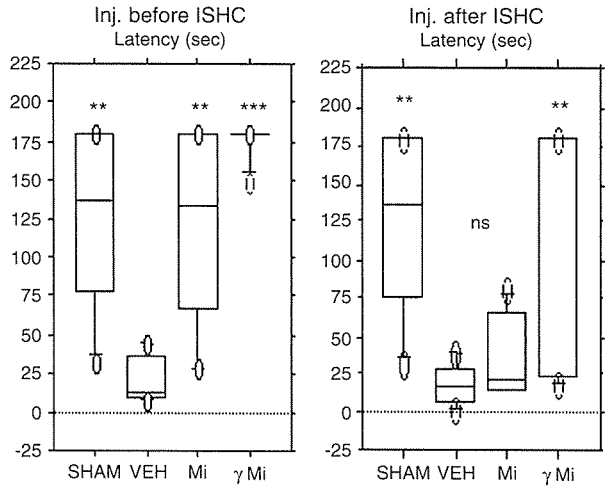

Figure 4 The effects of microglia on the latency of the transient ischemic gerbils in the step-through passive avoidance task. The graphs show the results of passive avoidance task 7 days after ischemia. The mean retention latency of ISCH/Mi-PRE and ISCH/γMi-PRE animals was longer than that of ISCH/VEH-PRE animals. The mean retention latency of ISCH/γMi-POST animals was significantly longer than that of ISCH/VEH-POST animals, whereas that of ISCH/Mi-POST was not significantly longer. $^{**}P < 0.01$, $^{***}P < 0.001$, significantly different from ISCH/VEH with Scheffe's *post hoc* test for multiple pairwise comparisons ($n = 10$). Inj. before ISCH: intraarterial injection 24 h before ischemia treatment; Inj. after ISCH: intraarterial injection 24 h after ischemia treatment; SHAM: injection of culture medium into sham-ischemia treated animals; VEH: injection of culture medium into ischemia-treated animals; Mi: injection of nonstimulated microglia into ischemia-treated animals; γMi: injection of IFNγ-stimulated microglia into ischemia-treated animals.

PKH26-negative, IB4-positive cells. PKH26-negative, IB4-positive cells are either endogenous microglia/macrophage lineage cells or vascular endothelial cells.

Activated microglia share several characteristics with peripheral macrophages *in vitro*, but they display different phenotypes *in vivo* (Ling and Wong, 1993; Sawada *et al*, 1995, 1990, 1992). Several studies suggest a possible contribution of the invasion of blood-borne macrophages to delayed neuronal death after transient global ischemia (Lees, 1993). Our earlier studies showed that macrophages do not enter undamaged brain from the circulation (Imai *et al*, 1997). They might, however, enter the brain from the site of delayed neuronal death, where neovascularization and blood–brain barrier breakdown occur after ischemia (Kataoka *et al*, 2000). In our ischemia model, PKH26-labeled peritoneal macrophages did not enter the brain from the circulation. Therefore, IB4-positive, PKH26-negative cells migrating to the ischemic CA1 layer are likely to be endogenous microglia. Most of the migrating cells in the CA1 area were not endogenous microglia, but rather exogenous microglia. It is possible that isolated microglia from the mixed brain cultures are already activated (Streit, 1993) and so migrate to the ischemic lesion more rapidly than endogenous microglia.

Injection of exogenous microglia increased the number of surviving CA1 neurons after transient global ischemia, even when microglia were injected after the ischemic insult. The microglial neuroprotective effect also prevented an ischemia-induced learning impairment. In this and previous studies, we have shown that microglia isolated from a newborn mixed brain culture express both BDNF and GDNF, and intraarterial injection of microglia increases the presence of these neurotrophic factors in the ischemic hippocampus (Suzuki *et al*, 2001). Beyer *et al* (2000) reported that phagocytosis of Latex beads induced a microglial amoeboid morphology but did not increase immunologically relevant molecules. Microglia that phagocytose PKH26 would have similar properties as those that phagocytose Latex beads. PKH26 phagocytosis labeling did not affect microglial expression of neurotrophic factors and neuroprotection (data not shown). Upregulation of both neurotrophic factors in damaged brain is crucial for protection from neurodegeneration (Ebadi *et al*, 1997). The association between exogenous microglia at the lesion site and decreased cell death, increased neurotrophic factor expression, and improved learning ability after ischemic injury leads us to conclude that microglia have a protective effect rather than a toxic effect, on neurons under ischemic conditions.

We examined the time course of hippocampal BDNF and GDNF expression after transient global ischemia, and investigated the effect of exogenous microglia on the expression of these neurotrophic factors. In normal CA1 neurons, the expression of both neurotrophic factors was preserved; however, their immunoreactivity was reduced 2 h after ischemia and then increased in a time-dependent manner. Seven days after ischemia, the main sources of BDNF were damaged CA1 neurons, endogenous microglia, and reactive astrocytes. Reactive astrocytes were excluded as the source of GDNF because they do not express GDNF in our model. The BDNF results are consistent with previous studies (Kokaia *et al*, 1996; Lee *et al*, 2002), whereas the GDNF results are inconsistent with a study by Miyazaki *et al* (2001). They reported that GDNF expression in the hippocampal CA1 region increased between 3 and 24 h after ischemia, and then declined to baseline levels. In their model, in which rats are subjected to a transient global ischemia induced by four-vessel occlusion, reactive astrocytes express GDNF. The discrepancy in the results between the two studies is possibly because of the use of different animal models of ischemia. In the present study, injection of microglia prevented the decrease in BDNF and GDNF expression in the hippocampus immediately after ischemia, and later increased the expression of these trophic factors. CA1 neurons,